The Inflation Technique for Causal Inference with Latent Variables

Elie Wolfe,[1, *] Robert W. Spekkens,[1, †] and Tobias Fritz[1, 2, ‡]

[1]*Perimeter Institute for Theoretical Physics, Waterloo, Ontario, Canada, N2L 2Y5*
[2]*Max Planck Institute for Mathematics in the Sciences, Leipzig, Germany*

(Dated: August 5, 2016)

The fundamental problem of causal inference is to determine whether or not a given probability distribution over observed variables is compatible with some causal structure (which may incorporate latent variables). It is therefore valuable to be able to derive inequalities whose violation by a distribution witnesses the incompatibility of that distribution with the given causal structure. We term these causal compatibility inequalities. Prominent examples are Bell inequalities and Pearl's instrumental inequality. We here introduce a technique for deriving such inequalities for arbitrary causal structures. It consists of blowing up or *inflating* the causal structure of interest to a new causal structure that can contain multiple copies of each of the original variables. By construction, any causal compatibility inequality on the inflated structure can be translated into one for the original structure. Because inflation often introduces novel d-separation relations, it often generates easy opportunities for such translations. We demonstrate the technique's power by numerically deriving all of the constraints that it implies for a particular concrete example—an inflation of the so-called triangle scenario —obtaining a set of causal compatibility inequalities that are provably stronger than those derived from other techniques. Given a *specific* probability distribution and a causal structure, our technique provides an efficient means of witnessing their incompatibility. Finally, we discuss how to identify, among the causal compatibility inequalities that the technique yields, those that remain necessary conditions on compatibility even for quantum (and post-quantum) generalizations of the notion of a causal model.

---

[*] ewolfe@perimeterinstitute.ca
[†] rspekkens@perimeterinstitute.ca
[‡] fritz@mis.mpg.de

CONTENTS

I. INTRODUCTION

Given a joint probability distribution of some observed variables, the problem of **causal inference** is to determine which hypotheses about the causal mechanism can explain the given distribution. Here, a causal mechanism may comprise both causal relations among the observed variables, as well as among these and a number of unobserved variables. Causal inference problems arise in a wide variety of scientific disciplines, from sussing out biological pathways to enabling machine learning [1–4]. A closely related type of problem is to determine, for a given set of causal relations, the set of all distributions of observed variables that can be generated from them. A special case of both problems is the following decision problem: given a probability distribution and a hypothesis about the causal relations, determine whether the two are compatible: could the given distribution have been generated by the hypothesized causal relations? This is the problem that we focus on. We develop necessary conditions for a given distribution to be compatible with a given hypothesis about the causal relations.

In the simplest setting, the causal hypothesis consists of a directed acyclic graph (DAG) *all* of whose nodes correspond to observed variables. In this case, obtaining a verdict on the compatibility of a given distribution with the causal hypothesis is simple: the compatibility holds if and only if the distribution is Markov with respect to the DAG, which is to say that the distribution features all of the conditional independence relations asserted by d-separation with respect to the DAG. The compatible DAGs can be determined algorithmically solely from the distribution [1].

A significantly more difficult case is when one considers a causal hypothesis which consists of a DAG whose nodes include **latent** (i.e., unobserved) variables, so that the set of observed variables is a strict subset of the nodes of the DAG. This case occurs, e.g., in situations where one needs to deal with the possible presence of unobserved confounders, and is particularly relevant for experimental design in statistics.

It is useful to distinguish two varieties of this problem: (i) the causal hypothesis specifies that the latent variables are discrete and of a particular cardinality[1], and (ii) the nature of the latent variables is arbitrary.

Consider the first variety of causal inference problem, where the cardinalities of the latent variables are all finite. Then the mathematical problem which one must solve to infer the distributions that are compatible with the hypothesis is a quantifier elimination problem for some finite number of quantifiers, as follows. The probabilities making up the distribution over the observed variables can all be expressed as functions of the parameters specifying the conditional probabilities of each node given its parents, many of which involve latent variables. If one can eliminate these unobservable parameters, then one obtains constraints that refer exclusively to the probability distribution over the observed variables. This is a *nonlinear* quantifier elimination problem. While the Tarski-Seidenberg theorem provides an *in principle* algorithm for an exact solution, the computational complexity of such quantifier elimination techniques is too large to be practical, except in particularly simple scenarios [5]. Techniques for finding approximate solutions to nonlinear quantifier elimination may help [6].

The second variety of causal inference problem, where the latent variables are arbitrary, is even more difficult, but also the case that has been the focus of most research and that motivates the present work. It is conceivable that inference problems of this variety can be expressed as quantifier elimination problems as well. This would be the case, for instance, if one could show that latent variables of a certain finite cardinality (as opposed to arbitrary latent variables) are sufficient to generate all the distributions compatible with that DAG[2]. At present, the problem of finding an algorithm for deciding compatibility in this second case—let alone an efficient algorithm—remains open. Even if it *is* possible to achieve a reduction to the case of latent variables with finite cardinality, one would still be faced with the above nonlinear quantifier elimination problem. As such, heuristic techniques for obtaining nontrivial constraints, such as the one presented in this work, are more important in practice.

If one allows for latent variables, then the condition that all of the conditional independence relations among the observed variables should be explained by the structure of the DAG is still a necessary condition for compatibility of a DAG with a given distribution, but in general it is no longer a sufficient condition for compatibility. Historically, the insufficiency of the conditional independence relations for causal inference in the presence of latent variables was first noted by Bell in the context of the hidden variable problem in quantum physics [8]. Bell considered an experiment for which considerations from relativity theory implied a very particular causal structure, and he derived an inequality that any distribution compatible with this structure, and compatible with certain constraints imposed by quantum theory, must satisfy. Bell also showed that this inequality was violated by distributions generated from entangled quantum states with particular choices of incompatible measurements. Later work, by Clauser, Horne, Shimony and Holte (CHSH) [9] showed how to derive inequalities directly from the causal structure. The CHSH inequality was the first example of a compatibility condition that appealed to the strength of the correlations rather than simply the conditional independence relations inherent therein. Since then, many generalizations of the CHSH inequality have been derived for the same sort of causal structure [10]. The idea that such work is best understood as a contribution to the field of causal inference has only recently been put forward [11–14], as has the idea that techniques developed by researchers in the foundations of quantum theory may be usefully adapted to causal inference[3].

Subsequent to Bell's work, Pearl derived an inequality, called the **instrumental inequality** [22], which provides a necessary condition for the compatibility of a distribution with a causal structure known as the *instrumental scenario* that applies, for instance, to certain kinds of noncompliance in drug trials. Steudel and Ay [23] later derived an inequality which must hold whenever a distribution on n variables is compatible with a causal structure where no set of more than c variables has a common ancestor, for arbitrary $n, c \in \mathbb{N}$. Subsequent work has focused specifically on the case of $n = 3$ and $c = 2$, a causal structure that has been called the Triangle scenario [12, 24].

Recently, Henson, Lal and Pusey [13] have found a sufficient condition for a DAG to be *interesting*, by which they mean that conditional independence relations do not exhaust the set of constraints on the compatibility of a joint distribution over observed variables with the DAG. They also presented a catalogue of all potentially interesting DAGs having six or fewer nodes in [13, App. E], of which all but three were shown to be indeed interesting. The Bell scenario, the Instrumental scenario, and the Triangle scenario appear in the catalogue together with many others. Furthermore, the fraction of DAGs that are interesting increases as the total number of nodes increases. This highlights the need for moving beyond a case-by-case consideration of individual DAGs and for developing techniques for deriving constraints beyond conditional independence relations that can be applied to any interesting DAG, such as Shannon-type entropic

———————

[1] The cardinality of a variable is the number of possible values it can take.

[2] Rosset and Gisin [7] have an unpublished proof purporting to upper bound the cardinality of sufficiently general latent variables. We do not pursue the question here.

[3] The current article being another example of the phenomenon [6, 15–21].

inequalities [12, 16, 23–25]. They can be derived for a given DAG with relative ease, via exclusively linear quantifier elimination, since conditional independence relations are linear equations at the level of entropies. They also have the advantage that they apply regardless of the cardinality of the observable variables. Recent work has also looked at non-Shannon type inequalities, potentially further strengthening the entropic constraints [17, 26]. However, entropic techniques are still wanting, since the resulting inequalities are often rather weak. For example, they are not sensitive enough to distinguish uniquely-quantum correlations from their classical causal counterparts [12, 17].

Thus we here introduce a new technique for deriving necessary conditions for the compatibility of a distribution over observed variables with a given causal structure, which we term the *inflation technique*. Our technique is frequently capable of witnessing incompatibility when many other causal inference techniques fail. For example, in Example 2 of Sec. III-B we prove that the tripartite "W-type" distribution is incompatible with the Triangle scenario, despite the incompatibility being invisible to other causal inference tools such as conditional independence relations, Shannon-type [16, 24, 25] or non-Shanon-type entropic inequalities [17], or covariance matrices [18].

The inflation technique works roughly as follows. For a given DAG under consideration, one can construct many new DAGs, termed *inflations* of this DAG. These duplicate one or more of the nodes of the original DAG, while preserving their ancestral subgraph. Furthermore, the causal parameters that one adds to the inflated DAG are constrained to mirror those of the original DAG. We show that if the distributions over certain subsets of the observed variables are compatible with the original DAG, then the same distributions over certain copies of those subsets in the inflated DAG are compatible with the inflated DAG. Similarly, we show that any necessary condition for compatibility of a distribution with the inflated DAG translates into a necessary condition for compatibility with the original DAG. Thus standard techniques for deriving inequalities, applied to the inflated DAG, can be supplemented with the inflation technique to derive surprisingly strong inequalities for the original DAG. Concretely, we consider inequalities on the inflated DAG that are obtained from the *mere existence of a joint distribution* on the inflated DAG, supplemented with independence constraints arising from the inflated causal structure. We show how to derive a complete set of such inequalities by enumerating all facets of the associated **marginal polytope**. We also show how to compute a partial solution more efficiently by enumerating transversals of a certain hypergraph. Translating these back to the original DAG results in causal compatibility conditions in the form of nonlinear *polynomial inequalities*.

Together with the entropic techniques discussed above, our method is the first systematic tool for causal inference with latent variables that goes beyond observable conditional independence relations while not assuming any bounds on the cardinality of each latent variable. While our method can be used to systematically generate necessary conditions for compatibility with a given causal structure, we do not know whether the set of inequalities thus generated are also sufficient.

While we present our technique primarily as a tool for standard causal inference, we also briefly discuss applications to *quantum* causal models and causal models within generalized probabilistic theories [12–14, 16]. In particular, we discuss when our inequalities are also necessary conditions for a distribution over observed variables to be compatible with a given DAG within any generalized probabilistic theory.

II. BASIC DEFINITIONS OF CAUSAL MODELS AND COMPATIBILITY

A **causal model** consists of a pair of objects: a **causal structure** and a set of **causal parameters**. We define each in turn, but first recall the definition of directed acyclic graph (DAG). A DAG G consists of a finite set of nodes $\mathsf{Nodes}[G]$ and a set of directed edges $\mathsf{Edges}[G]$, where a directed edge is an ordered pair of nodes. Later, each node will carry a random variable and a directed edge between two nodes corresponds to the possibility of a direct causal influence from one variable to the other. In this way, the edges implement causal relations.

Our terminology for the causal relations between the nodes in a DAG is the standard one. The parents of a node X in G are defined as those nodes from which an outgoing edge terminates at X, i.e. $\mathsf{Pa}_G(X) = \{\, Y \mid Y \to X \,\}$. When the graph G is clear from the context, then we also omit the subscript. Similarly, the children of a node X in a given graph G are defined as those nodes at which edges originating at X terminate, i.e. $\mathsf{Ch}_G(X) = \{\, Y \mid X \to Y \,\}$. If $\boldsymbol{U}$ is a set of nodes, then we put $\mathsf{Pa}_G(\boldsymbol{U}) := \bigcup_{X \in \boldsymbol{U}} \mathsf{Pa}_G(X)$ and $\mathsf{Ch}_G(\boldsymbol{U}) := \bigcup_{X \in \boldsymbol{U}} \mathsf{Ch}_G(X)$. The **ancestors** of a set of nodes $\boldsymbol{U}$, denoted $\mathsf{An}_G(\boldsymbol{U})$, are defined as those nodes which have a directed *path* to some node in $\boldsymbol{U}$, *including the nodes in $\boldsymbol{U}$ themselves*[4]. Equivalently, $\mathsf{An}(\boldsymbol{U}) := \bigcup_{n \in \mathbb{N}} \mathsf{Pa}^n(\boldsymbol{U})$, where $\mathsf{Pa}^n(\boldsymbol{U})$ is inductively defined via $\mathsf{Pa}^0(\boldsymbol{U}) := \boldsymbol{U}$ and $\mathsf{Pa}^{n+1}(\boldsymbol{U}) := \mathsf{Pa}(\mathsf{Pa}^n(\boldsymbol{U}))$.

A **causal structure** is a DAG G that incorporates a distinction between two types of nodes: the set of observed nodes $\mathsf{ObservedNodes}[G]$, and the set of latent nodes $\mathsf{LatentNodes}[G]$. Following [13], we will depict the observed nodes

---

[4] Note the anti-colloquial self-inclusive definition of "ancestors" here. We use this definition so that any correlation between two variables can always be attributed to a common "ancestor", folding the case whence one variable is e.g. a parent of the other into the umbrella of common ancestry.

by triangles and the latent nodes by circles, as in Fig. 1. Henceforth, we will use the terms "DAG" and "causal structure" interchangeably, so that the specification of which variables are observed is considered to be part of the DAG. We denote the variable living at a node $X \in \mathsf{Nodes}[G]$ by the same letter X. Frequently we supplement the causal structure by a specification of the cardinalities of the observable variables at each node.

Moving towards causal models, we consider **causal parameters**. The set of causal parameters specifies, for each node X, the conditional probability distribution over the values of the random variable X, given the values of the variables $\mathsf{Pa}(X)$. In the case of root nodes, we have $\mathsf{Pa}(X) = \emptyset$, and the conditional distribution is a plain distribution. We write $P_{Y|X}$ for the conditional distribution of a variable Y given a variable X, while the particular conditional probability of the variable X taking the value x given that the variable Y takes the values y is denoted[5] $P_{Y|X}(y|x)$. Therefore, a given set of causal parameters has the form

$$\{P_{A|\mathsf{Pa}_G(A)} : A \in \mathsf{Nodes}[G]\}. \tag{1}$$

Finally, a **causal model** M consists of a causal structure together with a set of causal parameters,

$$M = (G, \{P_{A|\mathsf{Pa}_G(A)} : A \in \mathsf{Nodes}[G]\}).$$

A causal model specifies a joint distribution over all variables in the DAG via

$$P_{\mathsf{Nodes}[G]} = \prod_{A \in \mathsf{Nodes}[G]} P_{A|\mathsf{Pa}_G(A)}, \tag{2}$$

where $\prod$ denotes the usual product of functions, so that $(P_X \times P_Y)(x, y) := P_X(x)P_Y(y)$. A distribution $P_{\mathsf{Nodes}[G]}$ arises in this way if and only if it satisfies the Markov conditions associated to G.

The joint distribution over the observed variables is obtained from the joint distribution over all variables by marginalization over the latent variables

$$P_{\mathsf{ObservedNodes}[G]} = \sum_{\{X : X \in \mathsf{LatentNodes}[G]\}} P_{\mathsf{Nodes}[G]}, \tag{3}$$

where $\sum_X$ denotes marginalization over the variable X, so that $(\sum_X P_{XY})(y) := \sum_x P_{XY}(xy)$.

A given distribution of observed variables is said to be **compatible** with a given causal structure if there is some choice of the causal parameters that yields the given distribution via Eqs. (2) and (3). Furthermore, a given set of marginal distributions of various subsets of observed variables is said to be compatible with a given causal structure if and only if there exists a joint distribution of observed variables that yields these marginals and is compatible with the causal structure.

III. THE INFLATION TECHNIQUE FOR CAUSAL INFERENCE

A. Inflations of a causal model

We now introduce the notion of **an inflation of a causal model**. If a causal model lives on a DAG G, then an inflation of this model lives on an **inflation DAG** G'. There are many possible choices of inflation DAGs G' for a given G, forming a set $\mathsf{Inflations}[G]$. The choice of $G' \in \mathsf{Inflations}[G]$ is the only freedom in the inflation of a causal model. Once a choice is made, the set of parameters of the inflated model M' is fixed uniquely by the set of parameters of the original model M by a function $M' = \mathsf{Inflation}_{G \to G'}[M]$ that we define below. We begin by defining the condition under which a DAG G' is an inflation of a DAG G. This requires some preliminary definitions.

The **induced subgraph** of G obtained by restricting to a subset of nodes $\boldsymbol{V} \subseteq \mathsf{Nodes}[G]$ will be denoted $\mathsf{SubDAG}_G(\boldsymbol{V})$. It consists of the nodes $\boldsymbol{V}$ and those edges of G of which both endpoints are in $\boldsymbol{V}$. Of special importance to us is the **ancestral subgraph** of $\boldsymbol{V}$, denoted $\mathsf{AnSubDAG}_G(\boldsymbol{V})$, which is the subgraph induced by the ancestry of $\boldsymbol{V}$, $\mathsf{AnSubDAG}_G(\boldsymbol{V}) := \mathsf{SubDAG}_G(\mathsf{An}_G(\boldsymbol{V}))$.

In an inflation DAG G', every node behaves like a copy of a node of G. More precisely, the structure of being an inflation DAG also comprises a map $G' \to G$. We call the preimages of a node $A \in \mathsf{Nodes}[G]$ the *copies* of A in

----

[5] Although our notation suggests that all variables are discrete, we do not make this assumption: all our equations are straightforward to write down in proper measure-theoretic notation.

G', and denote them by $A_1, \ldots, A_k$. The subscript that indexes the copies is termed the **copy-index**. When two objects (e.g. nodes, sets of nodes, DAGs, etc...) are the same up to copy-indices, then we use $\sim$ to indicate this, as in $A_i \sim A_j \sim A$. Other examples are that $\boldsymbol{U} \sim \boldsymbol{U'}$ for sets of nodes $\boldsymbol{U} \subseteq \mathsf{Nodes}[G]$ and $\boldsymbol{U'} \subseteq \mathsf{Nodes}[G']$ if and only if $\boldsymbol{U'}$ contains exactly one copy of every node in $\boldsymbol{U}$, and similarly $\mathsf{SubDAG}_{G'}(\boldsymbol{U'}) \sim \mathsf{SubDAG}_G(\boldsymbol{U})$ means in addition that an edge is present between two nodes in $\boldsymbol{U'}$ if and only if it is present between the two associated nodes in $\boldsymbol{U}$.

In order to be an inflation, G' must locally mirror the causal structure of G:

Definition 1. *The DAG G' is said to be an **inflation** of the DAG G, that is, $G' \in \mathsf{Inflations}[G]$, if and only if for every node A_i in G', the ancestral subgraph of A_i in G' is equivalent, under removal of the copy-index, to the ancestral subgraph of A in G,*

$$G' \in \mathsf{Inflations}[G] \quad \textit{iff} \quad \forall A_i \in \mathsf{Nodes}[G'] : \mathsf{AnSubDAG}_{G'}(A_i) \sim \mathsf{AnSubDAG}_G(A). \tag{4}$$

To illustrate the notion of inflation, we consider the DAG of Fig. 1, which is called the *Triangle scenario* (for obvious reasons) and which has been studied by many authors [13 (Fig. E#8), 11 (Fig. 18b), 12 (Fig. 3), 24 (Fig. 6a), 27 (Fig. 1a), 28 (Fig. 8), 23 (Fig. 1b), 16 (Fig. 4b)]. Different inflations of the Triangle scenario are depicted in Figs. 2 to 6.
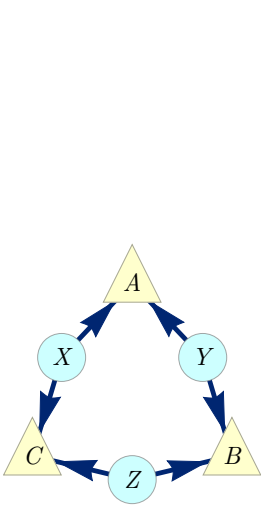

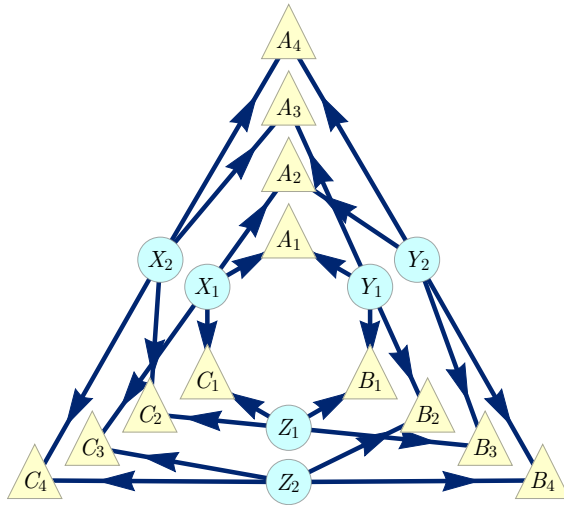FIG. 1. The causal structure of the Triangle scenario.

FIG. 2. An inflated DAG of the Triangle scenario where each latent node has been duplicated and each observable nodes node has been quadrupled. The four copies of each observable node correspond to the four possible choices of parentage in the inflated DAG.

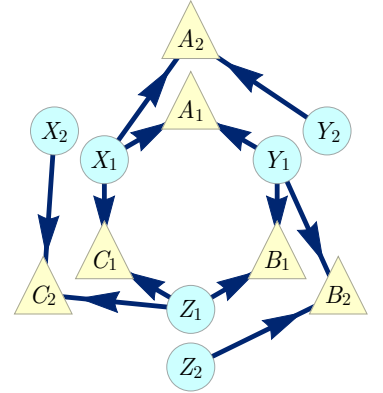FIG. 3. Another inflation of the Triangle scenario, also notably $\mathsf{AnSubDAG}_{(\mathrm{Fig.}\ 2)}(A_1A_2B_1B_2C_1C_2)$.

We now define the function $\mathsf{Inflation}_{G \to G'}$, that is, we specify how a causal model inflates.

Definition 2. *Consider causal models M and M' where $\mathsf{DAG}[M] = G$ and $\mathsf{DAG}[M'] = G'$ and such that G' is an inflation of G. The causal model M' is said to be the $G \to G'$ **inflation of** M, that is, $M' = \mathsf{Inflation}_{G \to G'}[M]$, if and only if for every node A_i in G', the manner in which A_i depends causally on its parents within G' is the same as the manner in which A depends causally on its parents within G. Noting that $A_i \sim A$ and that $\mathsf{Pa}_{G'}(A_i) \sim \mathsf{Pa}_G(A)$ by Eq. (4), one can formalize this condition as:*

$$\forall A_i \in \mathsf{Nodes}[G'] : P_{A_i | \mathsf{Pa}_{G'}(A_i)} = P_{A | \mathsf{Pa}_G(A)}. \tag{5}$$

It is clear that for given G, G' and M, this specifies a unique inflation model M', resulting in a well-defined function $\mathsf{Inflation}_{G \to G'}$.

To sum up then, the inflation of a causal model is a new causal model where (i) each variable in the original DAG may have counterparts in the inflated DAG with ancestral subgraphs mirroring those of the originals, and (ii) the manner in which a variable depends causally on its parents in the inflated DAG is given by the manner in which its counterpart in the original DAG depends causally on its parents. The operation of modifying a DAG and equipping the modified version with conditional probability distributions that mirror those of the original also appears in the *do*

calculus and *twin networks* of Pearl [1], and moreover bears some resemblance to the *adhesivity* technique used in deriving non-Shannon-type entropic inequalities (App. D).

We are now in a position to describe the key property of the inflation of a causal model, the one that makes it useful for causal inference. With notation as in Definition 2, let $P_{\boldsymbol{U}}$ and $P_{\boldsymbol{U}'}$ denote marginal distributions on some sets of nodes $\boldsymbol{U} \subseteq \mathsf{Nodes}[G]$ and $\boldsymbol{U}' \subseteq \mathsf{Nodes}[G']$, respectively. Then

$$\text{if} \quad \boldsymbol{U}' \sim \boldsymbol{U} \ \text{ and } \ \mathsf{AnSubDAG}_{G'}(\boldsymbol{U}') \sim \mathsf{AnSubDAG}_G(\boldsymbol{U}), \quad \text{then} \quad P_{\boldsymbol{U}'} = P_{\boldsymbol{U}}. \tag{6}$$

This follows from the fact that the probability distributions over $\boldsymbol{U}'$ and $\boldsymbol{U}$ depend only on their ancestral subgraphs and the parameters defined thereon, which by the definition of inflation are the same for $\boldsymbol{U}'$ and for $\boldsymbol{U}$. It is useful to have a name for those sets of observed nodes in G' which satisfy the antecedent of Eq. (6), that is, for which one can find a copy-index-equivalent set in the original DAG G with a copy-index-equivalent ancestral subgraph. We call such subsets of the observed nodes of G' **injectable sets**,

$$\boldsymbol{U}' \in \mathsf{InjectableSets}[G']$$
$$\text{iff} \quad \exists \boldsymbol{U} \subseteq \mathsf{ObservedNodes}[G] \ : \ \boldsymbol{U}' \sim \boldsymbol{U} \ \text{ and } \ \mathsf{AnSubDAG}_{G'}(\boldsymbol{U}') \sim \mathsf{AnSubDAG}_G(\boldsymbol{U}). \tag{7}$$

Similarly, those sets of observed nodes in the original DAG G which satisfy the antecedent of Eq. (6), that is, for which one can find a corresponding set in the inflated DAG G' with a copy-index-equivalent ancestral subgraph, we describe as **images of the injectable sets**,

$$\boldsymbol{U} \in \mathsf{ImagesInjectableSets}[G]$$
$$\text{iff} \quad \exists \boldsymbol{U}' \subseteq \mathsf{ObservedNodes}[G'] \ : \ \boldsymbol{U}' \sim \boldsymbol{U} \ \text{ and } \ \mathsf{AnSubDAG}_{G'}(\boldsymbol{U}') \sim \mathsf{AnSubDAG}_G(\boldsymbol{U}). \tag{8}$$

Clearly, $\boldsymbol{U} \in \mathsf{ImagesInjectableSets}[G]$ iff $\exists \boldsymbol{U}' \subseteq \mathsf{InjectableSets}[G']$ such that $\boldsymbol{U} \sim \boldsymbol{U}'$.

For example in the inflation of the Triangle scenario depicted in Fig. 3, the set of observed nodes $\{A_1 B_1 C_1\}$ is injectable because its ancestral subgraph is equivalent up to copy-indices to the ancestral subgraph of $\{ABC\}$ in the original DAG, and the set $\{A_2 C_1\}$ is injectable because its ancestral subgraph is equivalent to that of $\{AC\}$ in the original DAG. A set of nodes in the inflated DAG can only be injectable if it contains at most one copy of any node from the original DAG. More strongly, it can only be injectable if its ancestral subgraph contains at most one copy of any node from the original DAG.

Thus, in Fig. 3, $\{A_1 A_2 C_1\}$ is not injectable because it contains two copies of A, and $\{A_2 B_1 C_1\}$ is not injectable because its ancestral subgraph contains two copies of Y. The fact that the sets $\{A_1 B_1 C_1\}$ and $\{A_2 C_1\}$ are injectable implies, via Eq. (6), that the marginals on each of these in the inflation model are precisely equal to the marginals on their counterparts, $\{ABC\}$ and $\{AC\}$, in the original causal model, so that $P_{A_1 B_1 C_1} = P_{ABC}$ and $P_{A_2 C_1} = P_{AC}$.

It is useful to express Eq. (6) in the language of injectable sets,

$$P_{\boldsymbol{U}'} = P_{\boldsymbol{U}} \quad \text{if} \quad \boldsymbol{U}' \sim \boldsymbol{U} \ \text{ and } \ \boldsymbol{U}' \in \mathsf{InjectableSets}[G']. \tag{9}$$

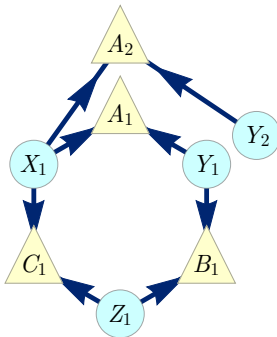FIG. 4. A rather simple inflation of the Triangle scenario, also notably $\mathsf{AnSubDAG}_{(Fig.\ 3)}(A_1 A_2 B_1 C_1)$.
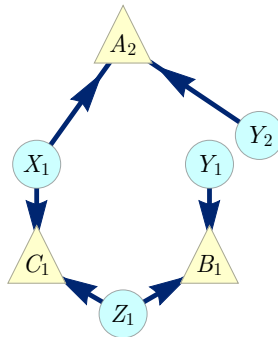
FIG. 5. An even simpler inflation of the Triangle scenario, also notably $\mathsf{AnSubDAG}_{(Fig.\ 4)}(A_2 B_1 C_1)$.
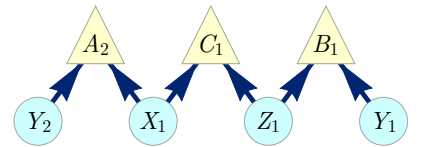
FIG. 6. A different drawing of Fig. 5. Despite not containing the original scenario, this is a valid inflation per Eq. (4).

B. Witnessing incompatibility

Finally, we can explain why inflation is relevant for deciding whether a distribution is compatible with a causal structure. For a family of marginal distributions $\{P_U : U \in \mathsf{ImagesInjectableSets}[G]\}$ to be compatible with G, there must be a causal model M that yields a joint distribution with this family as its marginals. Looking at the inflation model $M' = \mathsf{Inflation}_{G \to G'}[M]$, Eq. (9) implies that M' has the corresponding family of marginals given by $\{P_{U'} : U' \in \mathsf{InjectableSets}[G']\}$ with $P_{U'} = P_U$ for $U' \sim U$, and thus this family is compatible with G'.

The same considerations apply for subcollections of injectable sets:

Lemma 3. *Let G' an inflation DAG of G. Let $S' \subseteq \mathsf{InjectableSets}[G']$ be a collection of injectable sets, and let $S \subseteq \mathsf{ImagesInjectableSets}[G]$ be the images of this collection. If the family of marginal distributions $\{P_U : U \in S\}$ is compatible with G, then the corresponding family of marginal distributions $\{P_{U'} : U' \in S'\}$ — defined via $P_{U'} = P_U$ for $U' \sim U$ — is compatible with G'.*

We have thereby related a question about compatibility with the original causal structure to one about compatibility with the inflated causal structure. If one can show that the new compatibility question on G' is answered in the negative, then one can infer that the original question is answered in the negative as well. Some simple examples serve to illustrate the idea.

Example 1: **Witnessing the incompatibility of perfect three-way correlation with the Triangle scenario.**
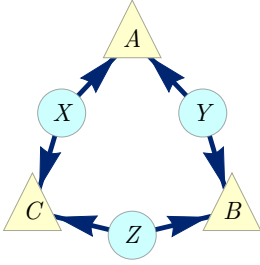

FIG. 7. The causal structure of the Triangle scenario. (Repeat of Fig. 1.)
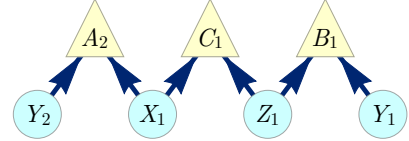
FIG. 8. A relevant inflation of the Triangle scenario. (Repeat of Fig. 6.)

Consider the following causal inference problem. One is given a joint distribution over three binary variables, P_{ABC}, where the marginal on each variable is uniform and the three are perfectly correlated,

$$P_{ABC} = \frac{[000] + [111]}{2}, \quad \text{i.e.,} \quad P_{ABC}(abc) = \begin{cases} \frac{1}{2} & \text{if } a{=}b{=}c, \\ 0 & \text{otherwise,} \end{cases} \tag{10}$$

and one would like to determine whether it is compatible with the Triangle scenario, that is, the DAG depicted in Fig. 7. The sum-over-brackets notation in Eq. (10) is a shorthand for indicating discrete probability distributions: the coefficient of each bracketed tuple indicates the probability of that particular joint outcome.

Since there are no conditional independence relations among the observed variables in the Triangle scenario, there is no opportunity for ruling out the distribution on the grounds that it fails to satisfy the required conditional independences.

To solve this problem, we consider the inflation of the Triangle scenario to the DAG depicted in Fig. 8. The injectable sets in this case include $\{A_2 C_1\}$ and $\{B_1 C_1\}$. We therefore consider the marginals on these sets.

Clearly, the given distribution can only be compatible with the Triangle hypothesis if the following pair of marginals of the given distribution are compatible with the Triangle hypothesis:

$$P_{AC} = P_{BC} = \frac{[00] + [11]}{2}.$$

But by Lemma 3, this compatibility holds only if the following pair of marginals is compatible with the inflation of Fig. 8,

$$P_{A_2 C_1} = P_{B_1 C_1} = \frac{[00] + [11]}{2}.$$

It is not difficult to see that the latter pair of marginals is *not* compatible with our inflated DAG. It suffices to note that the only joint distribution that exhibits perfect correlation between A_2 and C_1 and between B_1 and C_1 also exhibits perfect correlation between A_2 and B_1. But A_2 and B_1 have no common ancestors and hence must be marginally independent in the inflated DAG.

We have therefore certified that the joint distribution P_{ABC} of Eq. (10) is not compatible with the Triangle causal structure, recovering a result originally proven by Steudel and Ay [23].

Example 2: **Witnessing the incompatibility of the W-type distribution with the Triangle scenario**
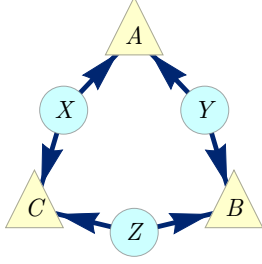

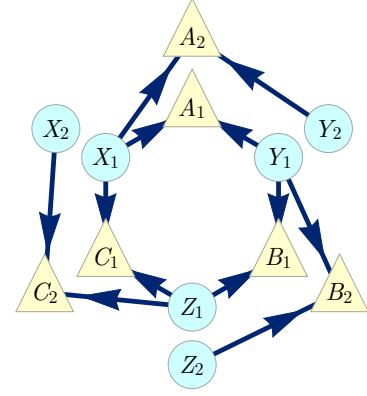FIG. 9. The causal structure of the Triangle scenario. (Repeat of Fig. 1.)

FIG. 10. A relevant inflation of the Triangle scenario. (Repeat of Fig. 3.)

Consider another causal inference problem concerning the Triangle scenario, namely, that of determining whether the hypothesis of the Triangle DAG is compatible with a joint distribution P_{ABC} of the form

$$P_{ABC} = \frac{[100] + [010] + [001]}{3}, \quad \text{i.e.,} \quad P_{ABC}(abc) = \begin{cases} \frac{1}{3} & \text{if } a+b+c=1, \\ 0 & \text{otherwise.} \end{cases} \tag{11}$$

We call this the W-type distribution[6].

To settle the compatibility question, we consider the inflated DAG of Fig. 10. The injectable sets in this case include $\{A_1 B_1 C_1\}$, $\{A_2 C_1\}$, $\{B_2 A_1\}$, $\{C_2 B_1\}$, $\{A_2\}$, $\{B_2\}$ and $\{C_2\}$.

Therefore, we turn our attention to determining whether the marginals of the W-type distribution on the images of these injectable sets are compatible with the Triangle hypothesis. These marginals are:

$$P_{ABC} = \frac{[100] + [010] + [001]}{3}, \tag{12}$$

$$P_{AC} = P_{BA} = P_{CB} = \frac{[10] + [01] + [00]}{3}, \tag{13}$$

$$P_A = P_B = P_C = \frac{2}{3}[0] + \frac{1}{3}[1]. \tag{14}$$

But by Lemma 3, this compatibility holds only if the corresponding set of marginals is compatible with the inflated DAG depicted in Fig. 10:

$$P_{A_1 B_1 C_1} = \frac{[100] + [010] + [001]}{3}, \tag{15}$$

$$P_{A_2 C_1} = P_{B_2 A_1} = P_{C_2 B_1} = \frac{[10] + [01] + [00]}{3}, \tag{16}$$

$$P_{A_2} = P_{B_2} = P_{C_2} = \frac{2}{3}[0] + \frac{1}{3}[1]. \tag{17}$$

---

[6] Because its correlations are reminiscent of those one obtains for the quantum state appearing in [29], called the *W state*.

Eq. (16) implies that $C_1=0$ whenever $A_2=1$. It also implies that $A_1=0$ whenever $B_2=1$, and that $B_1=0$ whenever $C_2=1$,

$$
\begin{aligned}
A_2=1 &\implies C_1=0, \\
B_2=1 &\implies A_1=0, \\
C_2=1 &\implies B_1=0.
\end{aligned}
\tag{18}
$$

Our inflated DAG is such that A_2, B_2 and C_2 have no common ancestor and consequently, they are all marginally independent in any distribution consistent with this inflated DAG. This fact, together with Eq. (17), implies that

$$\text{Sometimes}\quad A_2=1 \text{ and } B_2=1 \text{ and } C_2=1. \tag{19}$$

Finally, Eq. (18) together with Eq. (19) entails

$$\text{Sometimes}\quad A_1=0 \text{ and } B_1=0 \text{ and } C_1=0. \tag{20}$$

This, however, contradicts Eq. (15). Consequently, the set of marginals described in Eqs. (15-17) are *not* compatible with the DAG of Fig. 10. By Lemma 3, this implies that the set of marginals described in Eqs. (12-14)—and therefore the W-type distribution of which they are marginals—is not compatible with the Triangle scenario.

To our knowledge, this has not been demonstrated previously. In fact, the incompatibility of the W-type distribution with the Triangle scenario cannot be derived via any of the following pre-existing causal inference techniques:

1. Checking conditional independence relations is not relevant here, as there are *no* conditional independence relations implied between any observable variables in the Triangle scenario.
2. The relevant Shannon-type entropic inequalities for the Triangle scenario have been classified, and they do not witness the incompatibility either [16, 24, 25].
3. Moreover, *no* entropic inequality can witness the W-type distribution as unrealizable. Weilenmann and Colbeck [17] have constructed an inner approximation to the entropic cone of the Triangle causal structure, and the W-distribution lies inside this. In other words, a distribution with the same entropic profile as the W-type distribution *can* arise from the Triangle scenario.
4. The newly-developed method of covariance matrix causal inference due to Åberg *et al.* [18], which gives tighter constraints than entropic inequalities for the Triangle scenario, also cannot detect the incompatibility.

Therefore, for this problem at least, the inflation technique appears to be more powerful. We have arrived at our incompatibility verdict by combining inflation with reasoning reminiscent of Hardy's version of Bell's theorem [30, 31]. Sec. IV-E will present a generalization of this kind of argument and its applications to causal inference.

Example 3: **Witnessing the incompatibility of PR-box correlations with the Bell scenario**

Bell's theorem [8–10, 32] concerns the question of whether the distribution obtained in an experiment involving a pair of systems that are measured at space-like separation is compatible with a causal structure of the form of Fig. 11. Here, the observed variables are $\{A, B, X, Y\}$, and Λ is a latent variable acting as a common cause of A and B. We shall term this causal structure the *Bell scenario*. While the causal inference formulation of Bell's theorem is not the traditional one, several recent articles have introduced and advocated this perspective [11 (Fig. 19), 13 (Fig. E#2), 14 (Fig. 1), 24 (Fig. 1), 33 (Fig. 2b), 34 (Fig. 2)].
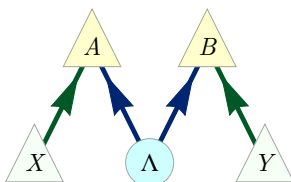

FIG. 11. The causal structure of the bipartite Bell scenario. The local outcomes A and B of Alice's and Bob's measurements is assumed to be a function of some latent common cause and their independent local experimental settings X and Y.
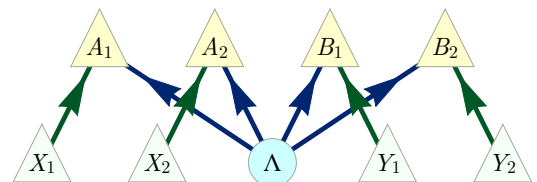

FIG. 12. An inflated DAG of the bipartite Bell scenario, where both local settings and outcome variables have been duplicated.

We consider the distribution $P_{ABXY} = P_{AB|XY} P_X P_Y$, where P_X and P_Y are arbitrary full-support distributions[7] over the binary variables X and Y, and

$$P_{AB|XY}(ab|xy) = \begin{cases} \frac{1}{2} & \text{if } a+b \equiv x \cdot y \pmod 2, \\ 0 & \text{otherwise,} \end{cases} \tag{21}$$

a conditional distribution that was discovered by Tsirelson [35] and later independently by Popescu and Rohrlich [36, 37]. It has become known in the field of quantum foundations as the *PR-box* after the latter authors.[8]

The Bell scenario implies nontrivial conditional independences among the observed variables, namely, $X \perp\!\!\!\perp Y$, $A \perp\!\!\!\perp Y|X$, and[9] $B \perp\!\!\!\perp X|Y$, as well as those that can be generated from these by the semi-graphoid axioms [11]. (In the context of a Bell experiment, where $\{X, A\}$ are space-like separated from $\{Y, B\}$, the conditional independences $A \perp\!\!\!\perp Y|X$, and $B \perp\!\!\!\perp X|Y$ encode the impossibility of sending signals faster than the speed of light.) It is straightforward to check that these conditional independence relations are respected by the P_{ABXY} resulting from Eq. (21). It is well-known that this distribution is nonetheless incompatible with the Bell scenario, for example since it violates the CHSH inequality. Here we prove this incompatibility via the inflation technique, using the inflation shown in Fig. 12.

We begin by noting that $\{A_1 B_1 X_1 Y_1\}$, $\{A_2 B_1 X_2 Y_1\}$, $\{A_1 B_2 X_1 Y_2\}$, $\{A_2 B_2 X_2 Y_2\}$, $\{X_1\}$, $\{X_2\}$, $\{Y_1\}$, and $\{Y_2\}$ are all injectable sets. By Lemma 3, it follows that any causal model that recovers P_{ABXY} inflates to a model that results in marginals

$$P_{A_1 B_1 X_1 Y_1} = P_{A_2 B_1 X_2 Y_1} = P_{A_1 B_2 X_1 Y_2} = P_{A_2 B_2 X_2 Y_2} = P_{ABXY}, \tag{22}$$

$$P_{X_1} = P_{X_2} = P_X, \qquad P_{Y_1} = P_{Y_2} = P_Y. \tag{23}$$

Using the definition of conditional probability, we infer that

$$P_{A_1 B_1 | X_1 Y_1} = P_{A_2 B_1 | X_2 Y_1} = P_{A_1 B_2 | X_1 Y_2} = P_{A_2 B_2 | X_2 Y_2} = P_{AB|XY}. \tag{24}$$

Because $\{X_1\}$, $\{X_2\}$, $\{Y_1\}$, and $\{Y_2\}$ have no common ancestor in the inflated DAG, these variables must be marginally independent in any distribution compatible with the inflated DAG. This applies in particular to the inflation model, so that $P_{X_1 X_2 Y_1 Y_2} = P_{X_1} P_{X_2} P_{Y_1} P_{Y_2}$. Given the assumption that the distributions P_X and P_Y are full support, it follows from Eq. (23) that

$$\text{Sometimes} \quad X_1 = 0, X_2 = 1, Y_1 = 0, Y_2 = 1. \tag{25}$$

On the other hand, from Eq. (24) together with the definition of PR-box, Eq. (21), we conclude that

$$\begin{aligned} X_1 = 0, Y_1 = 0 &\implies A_1 = B_1, \\ X_1 = 0, Y_2 = 1 &\implies A_1 = B_2, \\ X_2 = 1, Y_1 = 0 &\implies A_2 = B_1, \\ X_2 = 1, Y_2 = 1 &\implies A_2 \neq B_2. \end{aligned} \tag{26}$$

Combining this with Eq. (25), we obtain

$$\text{Sometimes} \quad A_1 = B_1, A_1 = B_2, A_2 = B_1, A_2 \neq B_2. \tag{27}$$

No values of A_1, A_2, B_1, B_2 can jointly satisfy these conditions—the first three entail perfect correlation between A_2 and B_2, while the fourth entails perfect anti-correlation—so we have reached a contradiction, showing that our original assumption of compatibility between P_{ABXY} and the Bell scenario must have been false.

The structure of this proof parallels that of standard proofs of the incompatibility of the PR-box with the Bell DAG. Standard proofs focus on a set of variables $\{A_0, A_1, B_0, B_1\}$ where A_x is the value of A when $X = x$ and B_y is the value of B when $Y = y$, and note that the distribution $\sum_\lambda P(A_0|\lambda)P(A_1|\lambda)P(B_0|\lambda)P(B_1|\lambda)P(\lambda)$ is a joint distribution over $\{A_0, A_1, B_0, B_1\}$ for which the marginals on pairs $\{A_0, B_0\}$, $\{A_0, B_1\}$, $\{A_1, B_0\}$ and $\{A_1, B_1\}$ are those predicted by the Bell DAG. Finally, the existence of such a joint distribution rules out the possibility of having

---

[7] In the literature on the Bell scenario, these variables are known as "settings". Generally, we may think of endogenous observable variables as settings, coloring them light green in the DAG figures. Settings variables are natural candidates for conditioning on.

[8] The PR-box is of interest because it represents a manner in which experimental correlations could deviate from the predictions of quantum theory while still being consistent with relativity.

[9] Recall that variables X and Y are conditionally independent given Z if $P_{X,Y|Z}(xy|z) = P_{X|Z}(x|z)P_{Y|Z}(y|z)$ for all z with $P_Z(z) > 0$. Such a conditional independence is denoted by $X \perp\!\!\!\perp Y \mid Z$.

$A_1=B_1, A_1=B_2, A_2=B_1$ but $A_2 \neq B_2$ and therefore shows that the PR Box correlations are incompatible with the Bell DAG [38, 39]. In light of our use of Eq. (25), our reasoning is really the same argument in disguise.

Appendix F shows that the inflation of Fig. 12, with the number of copies corresponding to the cardinality of X and Y, is enough to witness the incompatibility of any distribution that is indeed incompatible with the Bell scenario.

C. Deriving causal compatibility inequalities

The inflation technique can be used not only to witness the incompatibility of a given distribution with a given causal structure, but also to derive generally applicable necessary conditions that a distribution must satisfy to be compatible with the given causal structure. When these conditions are expressed as inequalities, we will refer to them as *causal compatibility inequalities*. Formally, we have:

Definition 4. *Let G be a causal structure and $S \subseteq \mathsf{ObservedNodes}[G]$. Let I_S denote an inequality that operates on a families of marginal distributions $\{P_{\boldsymbol{U}} : \boldsymbol{U} \in S\}$. Then I_S is a* **causal compatibility inequality for the causal structure** G *whenever it is satisfied by every family of distributions $\{P_{\boldsymbol{U}} : \boldsymbol{U} \in S\}$ that is compatible with G.*

While violation of a causal compatibility inequality witnesses the incompatibility of a distribution with the associated causal structure, the inequality being satisfied does not guarantee that the distribution is compatible with the causal structure. This is the sense in which it merely provides a *necessary* condition for compatibility.

The inflation technique is useful for deriving causal compatibility inequalities because of the following consequence of Lemma 3:

Corollary 5. *Suppose that G' is an inflation of G. Let $S' \subseteq \mathsf{InjectableSets}[G']$ be a family of injectable sets and $S \subseteq \mathsf{ImagesInjectableSets}[G]$ the images of members of S'. Let $I_{S'}$ be a causal compatibility inequality for G' operating on families $\{P_{\boldsymbol{U'}} : \boldsymbol{U'} \in S'\}$. Define an inequality I_S as follows: in the functional form of $I_{S'}$, replace every occurrence of a term $P_{\boldsymbol{U'}}$ by $P_{\boldsymbol{U}}$ for the unique $\boldsymbol{U} \in S$ with $\boldsymbol{U} \sim \boldsymbol{U'}$. Then I_S is a causal compatibility inequality for G operating on families $\{P_{\boldsymbol{U}} : \boldsymbol{U} \in S\}$.*

The proof is as follows. Suppose that the family $\{P_{\boldsymbol{U}} : \boldsymbol{U} \in S\}$ is compatible with G. By Lemma 3, it follows that the family $\{P_{\boldsymbol{U'}} : \boldsymbol{U'} \in S'\}$ where $P_{\boldsymbol{U'}} := P_{\boldsymbol{U}}$ for $\boldsymbol{U'} \sim \boldsymbol{U}$ is compatible with G'. Given that $I_{S'}$ is assumed to be a causal compatibility inequality for G', it follows that $\{P_{\boldsymbol{U'}} : \boldsymbol{U'} \in S'\}$ satisfies $I_{S'}$. But by the definition of I_S, its evaluation on $\{P_{\boldsymbol{U}} : \boldsymbol{U} \in S\}$ is equal to $I_{S'}$ evaluated on $\{P_{\boldsymbol{U'}} : \boldsymbol{U'} \in S'\}$. Since $\{P_{\boldsymbol{U'}} : \boldsymbol{U'} \in S'\}$ satisfies $I_{S'}$, it therefore follows that $\{P_{\boldsymbol{U}} : \boldsymbol{U} \in S\}$ satisfies I_S. Since $\{P_{\boldsymbol{U}} : \boldsymbol{U} \in S\}$ was an arbitrary family compatible with G, it follows that I_S is a causal compatibility inequality for G.

We now present some simple examples of causal compatibility inequalities for the Triangle scenario that one can derive from the inflation technique via Corollary 5.

Some terminology and notation will facilitate the description of these examples. We refer to a pair of nodes which do not share any common ancestor as being **ancestrally independent**. This corresponds to being d-separated by the empty set [1–4]. Given that the conventional notation for X and Y being d-separated by Z in the DAG G is $X \perp_G Y | Z$, we denote X and Y being ancestrally independent within G as $X \perp_G Y$. Generalizing to sets, $\boldsymbol{U} \perp_G \boldsymbol{V}$ indicates that no node in $\boldsymbol{U}$ shares a common ancestor with any node in $\boldsymbol{V}$ within the DAG G,

$$\boldsymbol{U} \perp_G \boldsymbol{V} \quad \text{iff} \quad \mathsf{An}_G(\boldsymbol{U}) \cap \mathsf{An}_G(\boldsymbol{V}) = \emptyset. \tag{28}$$

Furthermore, the notation $\boldsymbol{U} \perp_G \boldsymbol{V} \perp_G \boldsymbol{W}$ should be understood as indicating that $\boldsymbol{U} \perp_G \boldsymbol{V}$ and $\boldsymbol{V} \perp_G \boldsymbol{W}$ and $\boldsymbol{U} \perp_G \boldsymbol{W}$.

Example of a causal compatibility inequality expressed in terms of *correlators*

As in Example 1 of the previous section, consider the inflation of the Triangle scenario to the DAG depicted in Fig. 8. The injectable sets we make use of here are $\{A_2 C_1\}$, $\{B_1 C_1\}$, $\{A_2\}$, and $\{B_1\}$.

From Corollary 5, any causal compatibility inequality for the inflated DAG that operates on the marginal distributions of $\{A_2 C_1\}$, $\{B_1 C_1\}$, $\{A_2\}$, and $\{B_1\}$ will yield a causal compatibility inequality for the original DAG that can evaluated on the marginal distributions for $\{AC\}$, $\{BC\}$, $\{A\}$, and $\{B\}$. We begin, therefore by identifying a simple example of a causal compatibility inequality for the inflated DAG that is of this sort.

In our example, all of the observed variables are binary. For technical convenience, we assume that these take values in the set $\{-1, +1\}$, rather than taking values in the set $\{0, 1\}$ as was presumed in the last section.

We begin by noting that for *any* distribution on three binary variables $\{A_2 B_1 C_1\}$, that is, *regardless* of the causal structure in which they are embedded, the marginals on $\{A_2 C_1\}$, $\{B_1 C_1\}$ and $\{A_2 B_1\}$ satisfy the following inequality

for expectation values [40–44],

$$\langle A_2 C_1 \rangle + \langle B_2 C_1 \rangle - \langle A_2 B_1 \rangle \leq 1. \tag{29}$$

This is an example of a constraint on pairwise correlators that arises from the presumption that they are consistent with a joint distribution. (The problem of deriving such constraints is the so-called *marginal problem*, dicussed in detail in Sec. IV.)

But the DAG of Fig. 8 shows that A_2 and B_1 have no common ancestor and consequently any distribution compatible with the DAG must make A_2 and B_1 marginally independent. In terms of correlators, this can be expressed as

$$A_2 \perp B_1 \implies \langle A_2 B_1 \rangle = \langle A_2 \rangle \langle B_1 \rangle. \tag{30}$$

Substituting the latter equality into Eq. (29), we have

$$\langle A_2 C_1 \rangle + \langle B_2 C_1 \rangle \leq 1 + \langle A_2 \rangle \langle B_1 \rangle. \tag{31}$$

This is an example of a simple but nontrivial causal compatibility inequality for the DAG of Fig. 8.

Finally, by Corollary 5 and the fact that the DAG of Fig. 8 is an inflation of the Triangle scenario, we infer that

$$\langle AC \rangle + \langle BC \rangle \leq 1 + \langle A \rangle \langle B \rangle, \tag{32}$$

is a causal compatibility inequality for the Triangle scenario. This inequality expresses the fact that as long as A and B are not completely biased, there is a tradeoff between the strength of AC correlations and the strength of BC correlations.

Given the symmetry of the Triangle scenario under permutations and sign flips of A, B and C, it is clear that the image of inequality Eq. (32) under any such symmetry is also a valid causal compatibility inequality. Together, these inequalities imply monogamy[10] of correlations in the Triangle scenario with binary variables: if any two observed variables with unbiased marginals are perfectly correlated, then they are both uncorrelated with the third.

Example of a causal compatibility inequality expressed in terms of *entropic quantities*

One way to derive constraints that are independent of the cardinality of the observed variables is to express these in terms of the mutual information between observed variables rather than in terms of correlators. The inflation technique can also be applied to achieve this. To see how this works in the case of the Triangle scenario, consider again the inflated DAG of Fig. 8.

One can follow the same logic as in the preceding example, but starting from a different constraint on marginals. For any distribution on three variables $\{A_2 B_1 C_1\}$ of arbitrary cardinality (again, regardless of the causal structure in which they are embedded), the marginals on $\{A_2 C_1\}$, $\{B_1 C_1\}$ and $\{A_2 B_1\}$ satisfy the inequality [25, Eq. (29)]

$$I(A_2 : C_1) + I(C_1 : B_1) - I(A_2 : B_1) \leq H(C_1), \tag{33}$$

where $H(X)$ denotes the Shannon entropy of the distribution of X, and $I(X : Y)$ denotes the mutual information between X and Y with respect to the marginal on X and Y.

The fact that A_2 and B_1 have no common ancestor in the inflated DAG implies that in any distribution that is compatible with the inflated DAG, A_2 and B_1 are marginally independent. This is expressed entropically as the vanishing of their mutual information,

$$A_2 \perp B_1 \implies I(A_2 : B_1) = 0. \tag{34}$$

Substituting the latter equality into Eq. (33), we have

$$I(A_2 : C_1) + I(C_1 : B_1) \leq H(C_1). \tag{35}$$

This is another example of a nontrivial causal compatibility inequality for the DAG of Fig. 8.

By Corollary 5, it follows that

$$I(A : C) + I(C : B) \leq H(C), \tag{36}$$

———

[10] We are here using the term "monogamy" in the same sort of manner in which it is used in the context of entanglement theory [provide references]

is also a causal compatibility inequality for the Triangle scenario. This inequality was originally derived in [12]. Our rederivation in terms of inflation coincides with the proof found by Henson *et al.* [13].

Example of a causal compatibility inequality expressed in terms of *probabilities* of certain joint valuations

Consider the inflation of the Triangle scenario depicted in Fig. 10, with the injectable sets $\{A_1 B_1 C_1\}$, $\{A_1 B_2\}$, $\{B_1 C_2\}$, $\{A_1, C_2\}$, $\{A_2\}$, $\{B_2\}$, and $\{C_2\}$. We here derive a causal compatibility inequality under the assumption that the observed variables are binary, adopting the convention that they take values in $\{0, 1\}$.

We begin by noting that the following is a constraint that holds for any joint distribution of $\{A_1 B_1 C_1 A_2 B_2 C_2\}$, regardless of the causal structure,

$$P_{A_2 B_2 C_2}(111) \leq P_{A_1 B_1 C_1}(000) + P_{A_1 B_2 C_2}(111) + P_{B_1 C_2 A_2}(111) + P_{A_2 C_1 B_2}(111). \tag{37}$$

To prove this claim, it suffices to check that the inequality holds for each of the 2^6 deterministic assignments of values to $\{A_1 B_1 C_1 A_2 B_2 C_2\}$, from which the general case follows by linearity. A more intuitive proof will be provided in Sec. IV-E.

Next, we note that certain sets of variables have no common ancestors with other sets of variables in the inflated DAG, and we infer the marginal independence of the two sets, expressed now as a factorization of a joint distribution,

$$\begin{aligned}
A_1 B_2 \perp C_2 &\implies P_{A_1 B_2 C_2} = P_{A_1 B_2} P_{C_2}, \\
B_1 C_2 \perp A_2 &\implies P_{B_1 C_2 A_2} = P_{B_1 C_2} P_{A_2}, \\
A_2 C_1 \perp B_2 &\implies P_{A_2 C_1 B_2} = P_{A_2 C_1} P_{B_2}, \\
A_2 \perp B_2 \perp C_2 &\implies P_{A_2 B_2 C_2} = P_{A_2} P_{B_2} P_{C_2}.
\end{aligned} \tag{38}$$

Substituting these equations into Eq. (37), we obtain the polynomial inequality

$$P_{A_2}(1) P_{B_2}(1) P_{C_2}(1) \leq P_{A_1 B_1 C_1}(000) + P_{A_1 B_2}(11) P_{C_2}(1) + P_{B_1 C_2}(11) P_{A_2}(1) + P_{A_2 C_1}(11) P_{B_2}(1). \tag{39}$$

This, therefore, is a causal compatibility inequality for the DAG of Fig. 10. Finally, by Corollary 5, we infer that

$$P_A(1) P_B(1) P_C(1) \leq P_{ABC}(000) + P_{AB}(11) P_C(1) + P_{BC}(11) P_A(1) + P_{AC}(11) P_B(1) \tag{40}$$

is a causal compatibility inequality for the Triangle scenario.

What is distinctive about this inequality is that—through the presence of the term $P_{ABC}(000)$—it takes into account genuine three-way correlations. This inequality is strong enough to demonstrate the incompatibility of the W-type distribution of Eq. (11) with the Triangle scenario: for this distribution, the right-hand side of the inequality vanishes while the left-hand side does not.

Of the known techniques for witnessing the incompatibility of a distribution with a DAG or deriving necessary conditions for compatibility, the most straightforward is to consider the constraints implied by ancestral independences among the observed variables of the DAG. The constraints derived in the last two sections have all made use of this basic technique, but at the level of the inflated DAG rather than the original DAG. The constraints that one thereby infers for the original DAG reflect facts about its causal structure that cannot be expressed in terms of ancestral independences among its observed variables. The inflation technique manages to expose these facts in the ancestral independences among observed variables of the inflated DAG.

In the rest of this article, we shall continue to rely only on the ancestral independences among observed variables within the inflated DAG to infer compatibility constraints on the original DAG. Nonetheless, it is possible that the inflation technique can also amplify the power of *other* techniques that do not merely consider ancestral independences among the observed variables. We consider some prospects in Sec. V.

IV. SYSTEMATICALLY WITNESSING INCOMPATIBILITY AND DERIVING INEQUALITIES

In the examples from the previous section, the initial inequality—a constraint upon marginals that is independent of the causal structure—involves sets of observed variables that are *not* all injectable. Each of these sets can, however, be partitioned into disjoint subsets each of which *is* injectable whenever the partitioning represents ancestral independence in the inflated DAG. For instance, in the first example from the previous section, the set $\{A_2 B_1\}$ can be partitioned

into the singleton sets $\{A_2\}$ and $\{B_1\}$ which are ancestrally independent and each of which is injectable. It is useful to have a name for such sets of observed variables: we call them **pre-injectable**. So for a set of observable nodes $\boldsymbol{U}'$ in the inflated DAG G',

$$\boldsymbol{U}' \in \mathsf{PreInjectableSets}[G'] \quad \text{iff} \quad \exists\{\boldsymbol{U}_i \in \mathsf{InjectableSets}[G']\} \quad \text{s.t.} \quad \boldsymbol{U}' = \bigcup_i \boldsymbol{U}_i \quad \text{and} \quad \forall i \neq j : \boldsymbol{U}_i \perp \boldsymbol{U}_j. \tag{41}$$

For example, every injectable set is trivially a pre-injectable set. A pre-injectable set is *maximal* if it is not a proper subset of another pre-injectable set.

Because ancestral independence in the DAG implies statistical independence for any probability distribution compatible with the DAG, it follows that if $\boldsymbol{U}'$ is a pre-injectable set and $\boldsymbol{U}_1, \ldots, \boldsymbol{U}_n$ are the ancestrally independent components of $\boldsymbol{U}'$, then

$$P_{\boldsymbol{U}'} = P_{\boldsymbol{U}_1} \cdots P_{\boldsymbol{U}_n} \tag{42}$$

for any distribution compatible with G'. The situation, therefore, is this: for any constraint that one can derive for the marginals on the pre-injectable sets based on the existence of a joint distribution—and hence without reference to the causal structure—one can infer constraints that *do* refer to the causal structure by substituting within these constraints factorizations of the form of Eq. (42).

Thus the pre-injectable sets play a crucial role in linking the original DAG with the inflation DAG: they are precisely those sets of variables whose joint distributions in an inflation model are fully specified by the original causal model on the original DAG: they can be computed using Lemma 3 and Eq. (42). If the resulting family of marginal distributions on pre-injectable sets is not compatible with the existence of a joint distribution, then the original distribution is witnessed as causally incompatible with the original DAG. This is the formal argument underpinning all of the examples in Sec. III-B.

The problem of determining constraints on marginals follows from the existence of a joint distribution is known as the *marginal problem*. Thus, we can summarize the situation as follows: an inequality derived from the marginal problem, after applying the factorizations of Eq. (42), becomes a causal compatibility inequality for the inflated DAG. The latter inequality can then be converted into a polynomial causal compatibility inequality for the original DAG using Corollary 5. This section considers the problem of how to implement this procedure systematically.

We limit our attention to deriving causal compatibility inequalities expressed in terms of probabilities[11], as these are generally the most powerful. However, that the inflation technique can also be used to derive inequalities expressed in terms of entropies, as our second example from the previous section demonstrated. We show in Appendix D that the inflation technique implies the core lemma for deriving non-Shannon-type inequalities.

To obtain a complete solution of the marginal problem, one must determine all the facets of the **marginal polytope**, for which we discuss algorithms in Appendix A. Computing all these facets is computationally costly. It is therefore useful to also consider relaxations of the marginal problem that are less computationally burdensome by deriving valid linear inequalities which may or may not bound the marginal polytope tightly. We describe one such approach based on possibilistic Hardy-type paradoxes and the hypergraph transversal problem. This strategy requires the least computational effort, but is limited in that it only yields inequalities of a very particular form. We describe this approach in Sec. IV-E.

Preliminary to every strategy is the identification of the pre-injectable sets, so we begin with this problem.

A.   Identifying the pre-injectable sets

To identify the pre-injectable sets of an inflation DAG, we must first identify the injectable sets. This problem can be reduced to identifying the injectable pairs, because if all of the pairs in a set of nodes are injectable, then so too is the set itself. The latter claim is proven as follows. Let $\varphi : G' \to G$ be the projection map from the inflated DAG G' to the original DAG G, corresponding to removing the copy-indices. Then φ has the characteristic feature that it takes edges to edges: if $A \to B$ in G', then also $\varphi(A) \to \varphi(B)$ in G. Conversely, if $\varphi(A) \to \varphi(B)$ in G then also $A \to B$ in G'; this follows from the assumption that G' is an inflation of G. A set $\boldsymbol{U} \subseteq \mathsf{ObservedNodes}[G']$ is injectable if and only if the restriction of φ to the ancestors of $\boldsymbol{U}$ is an injective map. But now injectivity of a map means precisely that no two different elements of the domain get mapped to the same element of the codomain. So if $\boldsymbol{U}$ is injectable, then so is each of its two-element subsets; conversely, if $\boldsymbol{U}$ is not injectable, then φ maps two nodes among the ancestors of

---

[11] Or, for binary variables, equivalently in terms of correlators, as in the first example of Sec. III-C.
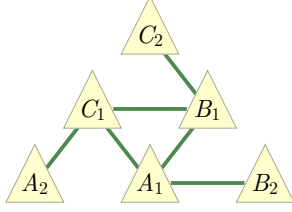
FIG. 13. The injection graph corresponding to the inflated DAG in Fig. 3, wherein a pair of nodes are adjacent iff they are pairwise injectable.
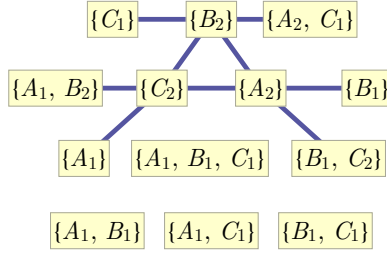

FIG. 14. The pre-injection graph corresponding to the inflated DAG in Fig. 3, wherein a pair of injectable sets are adjacent iff they are ancestrally independent.
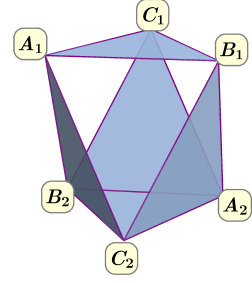

FIG. 15. The simplicial complex of pre-injectable sets for the inflation of Fig. 3. The 5 faces correspond to the maximal pre-injectable sets, namely $\{A_1 B_1 C_1\}$, $\{A_1 B_2 C_2\}$, $\{A_2 B_1 C_2\}$, $\{A_2 B_2 C_1\}$ and $\{A_2 B_2 C_2\}$.

U to the same node, which means that there are two nodes in the ancestry that differ only by copy index. Each of these two nodes must be an ancestor of at least some node in U; if one chooses two such descendants, then one gets a two-element subset of U such that φ is not injective on the ancestry of that subset, and therefore this two-element set of observed nodes is not injectable.

To enumerate the injectable sets, it is useful to encode certain features of the inflated DAG in an undirected graph which we call the **injection graph**. The nodes of the injection graph are the observed nodes of the inflated DAG, and a pair of nodes A_i and B_j share an edge if the pair $\{A_i B_j\}$ is injectable. For example, Fig. 13 shows the injection graph of the inflation of Fig. 3. The property noted above states that the injectable sets are precisely the cliques[12] of the injection graph. While for many other other applications only the maximal cliques are of interest, our application of the inflation technique requires knowledge of all nonempty cliques.

Given a list of the injectable sets, the pre-injectable sets can be read off from the **pre-injection graph**. The nodes of the pre-injection graph are taken to be the injectable sets in G', and two nodes share an edge if the associated injectable sets are ancestrally independent. Fig. 14 depicts an example. The pre-injectable sets correspond to the cliques of the pre-injection graph: the union of all the injectable sets that make up the nodes of a clique is a pre-injectable set, while the individual nodes already give us the partition into injectable sets relevant for the factorization relation of Eq. (42). For our purposes, it is sufficient to enumerate the maximal pre-injectable sets, so that one only needs to consider the maximal cliques of the pre-injection graph.

From Figs. 13 and 14, we easily infer the injectable sets and the maximal pre-injectable sets, as well as the partition of the maximal pre-injectable sets into ancestrally independent subsets, for the inflated DAG of Fig. 3 to be:

$$
\begin{array}{ccc}
\begin{array}{c}
\{A_1\},\ \{B_1\},\ \{C_1\}, \\
\{A_2\},\ \{B_2\},\ \{C_2\}, \\
\{A_1 B_1\},\ \{A_1 C_1\},\ \{B_1 C_1\}, \\
\{A_1 B_2\}.\ \{A_2 C_1\},\ \{B_1 C_2\}, \\
\{A_1 B_1 C_1\} \\
\underbrace{}_{\text{injectable sets}}
\end{array}
&
\begin{array}{c}
\{A_1 B_1 C_1\} \\
\{A_1 B_2 C_2\} \\
\{B_1 C_2 A_2\} \\
\{C_1 A_2 B_2\} \\
\{A_2 B_2 C_2\} \\
\underbrace{}_{\substack{\text{maximal} \\ \text{pre-injectable sets}}}
\end{array}
&
\begin{array}{c}
\{A_1 B_2\} \perp \{C_2\} \\
\{B_1 C_2\} \perp \{A_2\} \\
\{C_1 A_2\} \perp \{B_2\} \\
\{A_2\} \perp \{B_2\} \perp \{C_2\} \\
\underbrace{}_{\substack{\text{relevant} \\ \text{ancestral independences}}}
\end{array}
\end{array}
\tag{43}
$$

Using the ancestral independence relations, the marginal distributions for the maximal pre-injectable sets factorize in the manner described by the right-hand side of Eq. (38).

Having identified the pre-injectable sets together with the factorization relations implied by ancestral independences, we now discuss how to obtain constraints on the marginal distributions over the pre-injectable sets.

B. The marginal problem

For a given family of marginal distributions, each defined on a subset of the variables, determining whether there exists a joint probability distribution over the full set of variables from which all of these can be obtained as marginal

---

[12] A *clique* is a set of nodes in an undirected graph any two of which share an edge.

distributions is known as the *marginal problem*. For some of its history and for further references, see [25]; for a more modern account using the language of presheaves, see [45].

To specify such a problem, one must specify the full set of variables to be considered, denoted $\boldsymbol{X}$, together with a family of subsets of $\boldsymbol{X}$, denoted $(\boldsymbol{U}_1, \ldots, \boldsymbol{U}_n)$ and called **contexts**. A family of contexts can be visualized through the simplicial complex that they generate, as the example in Fig. 15 illustrates. Every joint distribution $P_{\boldsymbol{X}}$ defines a family of marginal distributions, $(P_{\boldsymbol{U}_1}, \ldots, P_{\boldsymbol{U}_n})$ through marginalization, $P_{\boldsymbol{U}_i} := \sum_{\boldsymbol{X} \setminus \boldsymbol{U}_i} P_{\boldsymbol{X}}$. A *marginal problem* concerns the converse inference. A family of distributions $(P_{\boldsymbol{U}_1}, \ldots, P_{\boldsymbol{U}_n})$ is given, and one wants to find conditions for when a joint distribution $\hat{P}_{\boldsymbol{X}}$ exists which reproduces given marginals, $P_{\boldsymbol{U}_i} = \sum_{\boldsymbol{X} \setminus \boldsymbol{U}_i} \hat{P}_{\boldsymbol{X}}$ for all i.

There is a simple necessary condition: in order for $\hat{P}_{\boldsymbol{X}}$ to exist, the marginals clearly must be consistent, in the sense that marginalizing $P_{\boldsymbol{U}_i}$ to the variables in $\boldsymbol{U}_i \cap \boldsymbol{U}_j$ results in the same distribution as marginalizing $P_{\boldsymbol{U}_j}$ to those variables. In many cases this is not sufficient; indeed, we have already seen examples of additional constraints, namely, the inequalities (29), (33) and (37) from Sec. III-C[13]. So what are the necessary and sufficient conditions?

To answer this question, it helps to realize two things:

- The set of possibilities for the distribution $P_{\boldsymbol{X}}$ is the convex hull of the deterministic assignments of values to $\boldsymbol{X}$ (the point distributions), and

- The map $P_{\boldsymbol{X}} \to (P_{\boldsymbol{U}_1}, \ldots, P_{\boldsymbol{U}_n})$, describing marginalization to each of the contexts in $(\boldsymbol{U}_1, \ldots, \boldsymbol{U}_n)$, is linear.

Hence the image of the set of possibilities for the distribution $P_{\boldsymbol{X}}$ under the map $P_{\boldsymbol{X}} \to (P_{\boldsymbol{U}_1}, \ldots, P_{\boldsymbol{U}_n})$ is exactly the convex hull of the deterministic assignments of values to $(\boldsymbol{U}_1, \ldots, \boldsymbol{U}_n)$ (more precisely, the deterministic assignments that are consistent where these contexts overlap). Since there are only finitely many such deterministic assignments, this convex hull is a polytope; it is called the **marginal polytope** [47]. Together with the above equations on coinciding submarginals, the facet inequalities of the marginal polytope form necessary and sufficient conditions for the marginal problem to have a solution.

As every facet enumeration problem, this can also be phrased as a problem of **linear quantifier elimination**. We illustrate this with the example of the marginal problem where $\boldsymbol{X} := \{A_1, A_2, B_1, B_2, C_1, C_2\}$ and the contexts are the maximal pre-injectable sets in Eq. (43). Besides normalization of probability, the only constraint on the probabilities making up the joint distribution is nonnegativity,

$$\forall a_1 a_2 b_1 b_2 c_1 c_2 : \ P_{A_1 A_2 B_1 B_2 C_1 C_2}(a_1 a_2 b_1 b_2 c_1 c_2) \geq 0. \tag{44}$$

We require the joint distribution to reproduce the marginal distribution on each context via

$$\forall a_1 b_1 c_1 : \ P_{A_1 B_1 C_1}(a_1 b_1 c_1) = \sum_{a_2 b_2 b_2} P_{A_1 A_2 B_1 B_2 C_1 C_2}(a_1 a_2 b_1 b_2 c_1 c_2),$$

$$\forall a_1 b_2 c_2 : \ P_{A_1 B_2 C_2}(a_1 b_2 c_2) = \sum_{a_2 b_1 c_1} P_{A_1 A_2 B_1 B_2 C_1 C_2}(a_1 a_2 b_1 b_2 c_1 c_2),$$

$$\forall a_2 b_1 c_2 : \ P_{A_2 B_1 C_2}(a_2 b_1 c_2) = \sum_{a_1 b_2 c_1} P_{A_1 A_2 B_1 B_2 C_1 C_2}(a_1 a_2 b_1 b_2 c_1 c_2), \tag{45}$$

$$\forall a_2 b_2 c_1 : \ P_{A_2 B_2 C_1}(a_2 b_2 c_1) = \sum_{a_1 b_1 c_2} P_{A_1 A_2 B_1 B_2 C_1 C_2}(a_1 a_2 b_1 b_2 c_1 c_2),$$

$$\forall a_2 b_2 c_2 : \ P_{A_2 B_2 C_2}(a_2 b_2 c_2) = \sum_{a_1 b_1 c_1} P_{A_1 A_2 B_1 B_2 C_1 C_2}(a_1 a_2 b_1 b_2 c_1 c_2).$$

If each variable is binary, then we have 64 inequalities and 40 equations, although the latter are not all independent.

The marginal problem is a linear system of equations and inequalities involving the unknown joint probabilities. The problem of quantifier elimination consists in finding an equivalent system of equations and inequalities that is satisfied if and only if the original system has a solution for the unknown probabilities. This requires eliminating 64 unknowns $P_{A_1 A_2 B_1 B_2 C_1 C_2}(a_1 a_2 b_1 b_2 c_1 c_2)$ for each of the 64 choices of the values $a_1, \ldots, c_2$. The resulting new system consists of the coinciding-submarginals equations together with the facet inequalities of the marginal polytope.

C. Witnessing incompatibility by non-sastisfiability of the marginal problem

Given a particular distribution (pertaining to variables on the original DAG) one can use the inflation DAG technique to test causal compatibility as follows. Using the factorization conditions implied by ancestral independences among

---

[13] Depending on how the contexts intersect with one another, this *may* be sufficient. A precise characterization for when this occurs has been found by Vorob'ev [46].

the variables in the maximal pre-injectable sets along with Lemma 3 one can infer the *distributions* over the maximal pre-injectable sets *pursuant* to the given original-scenario distribution; this was essentially the first step in each example in Sec. III-B.

Substituting explicit pre-injectable set distributions amounts to substituting numerical-values for the left-hand-side of every equality defined by the marginal problem, such as Eqs. (45). A single linear program can then assess whether the marginal problem equalities can be solved using nonnegative variables or not. If the inflation-DAG marginal problem *cannot be satisfied* then the given original-scenario distribution is witnessed as incompatible with the original DAG.

As satisfiability of the marginal problem can be resolved by a single linear program, testing specific distributions for causal compatibility with an inflation-DAG is computationally inexpensive. For instance, our technique is able to reproduce the result shown by Fritz [12, Theorem 2.16], that a particular distribution, inspired by the Bell example, is quantumly but not classically compatible with the Triangle scenario, using the rather complex inflation depicted in Fig. 2.

D. Causal compatibility inequalities via a complete solution of the marginal problem

A general scheme for deriving causal compatibility inequalities for a DAG can be summarized as follows. Choose an inflation of the DAG and identify the maximal pre-injectable sets thereon. Next, solve the marginal problem where the contexts are the maximal pre-injectable sets to obtain quantifier-free inequalities. Solving the marginal problem is therefore an instance of a facet enumeration problem. In Appendix A, we provide an overview of techniques for solving this problem.

By substituting into these inequalities the factorization conditions implied by ancestral independences among the variables in the maximal pre-injectable sets, one obtains causal compatibility inequalities for the inflated DAG. Finally, these can be converted into causal compatibility inequalities for the original DAG using Corollary 5.

As an example, we present all of the causal compatibility inequalities that one can derive for the Triangle scenario with binary observed variables using the inflation of Fig. 3.

Using the maximal pre-injectable sets identified in Eq. (43) as the contexts for the marginal problem, we solve the latter using the linear quantifier elimination method of Sec. IV. The facets of the marginal polytope can be characterized by a generating set of 64 inequalities. The full set of inequalities is obtained from the generating set by closing these under the action of two types of symmetry transformations: permutations of the observed variables and complementation (inversion) of the value for each variable. We then factorize the probabilities according to the ancestral independences in the inflated DAG, also identified in Eq. (43), to obtain a set of causal compatibility inequalities for the inflated DAG. Finally, these are converted to a generating set of causal compatibility inequalities for the original DAG using Corollary 5. Note, however, that there is no guarantee that each such conversion results in a nontrivial inequality at the level of the original DAG, where nontriviality means that the inequality is not true of all distributions, but is instead a consequence of the causal structure. Indeed, we find that only 37 of the inequalities in the generating set for the marginal polytope yield nontrivial causal compatability inequalities for the Triangle scenario. Moreover, it is likely to be the case that these 37 causal compatibility inequalities are not a minimal generating set, where a minimal generating set is defined as one such that, for every inequality, there is a distribution that violates it while satisfying all of the others. We present our generating set of causal compatibility inequalities for the Triangle scenario below. A machine-readable version of this set of inequalities may be found in Appendix E. A star next to the index of an inequality indicates that the inequality can also be derived by considering the possibilisitc marginal

problem per Sec. IV-E in lieu of solving the usual (probabilistic) marginal problem.

$(\#1^*)$: $\quad 0 \le 1 + \langle B \rangle \langle C \rangle + \langle AB \rangle + \langle AC \rangle$

$(\#2)$: $\quad 0 \le 2 + \langle A \rangle \langle B \rangle \langle C \rangle - \langle C \rangle \langle AB \rangle - 2 \langle AC \rangle$

$(\#3^*)$: $\quad 0 \le 3 + \langle A \rangle - \langle B \rangle + \langle C \rangle + \langle B \rangle \langle C \rangle + \langle A \rangle \langle B \rangle \langle C \rangle + \langle AB \rangle - \langle C \rangle \langle AB \rangle + 3 \langle AC \rangle - \langle B \rangle \langle AC \rangle$

$(\#4^*)$: $\quad 0 \le 3 + \langle A \rangle - \langle B \rangle + \langle C \rangle + \langle B \rangle \langle C \rangle - \langle A \rangle \langle B \rangle \langle C \rangle + \langle AB \rangle + \langle C \rangle \langle AB \rangle + 3 \langle AC \rangle - \langle B \rangle \langle AC \rangle$

$(\#5)$: $\quad 0 \le 3 + \langle B \rangle - \langle A \rangle \langle B \rangle + \langle A \rangle \langle C \rangle + \langle A \rangle \langle B \rangle \langle C \rangle + \langle AB \rangle + \langle C \rangle \langle AB \rangle - \langle B \rangle \langle AC \rangle - 2 \langle BC \rangle$

$(\#6)$: $\quad 0 \le 3 + \langle B \rangle + \langle A \rangle \langle C \rangle + \langle A \rangle \langle B \rangle \langle C \rangle - \langle C \rangle \langle AB \rangle - 2 \langle AC \rangle - \langle B \rangle \langle AC \rangle - 2 \langle BC \rangle$

$(\#7)$: $\quad 0 \le 3 + \langle B \rangle + \langle A \rangle \langle B \rangle - \langle A \rangle \langle C \rangle - \langle A \rangle \langle B \rangle \langle C \rangle + \langle AB \rangle + \langle C \rangle \langle AB \rangle + \langle B \rangle \langle AC \rangle - 2 \langle BC \rangle$

$(\#8^*)$: $\quad 0 \le 3 + \langle A \rangle + \langle B \rangle + \langle A \rangle \langle B \rangle + \langle C \rangle + \langle A \rangle \langle C \rangle + \langle B \rangle \langle C \rangle - \langle A \rangle \langle B \rangle \langle C \rangle + 2 \langle AB \rangle + \langle C \rangle \langle AB \rangle + 2 \langle AC \rangle + \langle B \rangle \langle AC \rangle + 2 \langle BC \rangle + \langle A \rangle \langle BC \rangle - \langle ABC \rangle$

$(\#9^*)$: $\quad 0 \le 3 + \langle A \rangle + \langle B \rangle - \langle A \rangle \langle B \rangle + \langle C \rangle + \langle A \rangle \langle C \rangle + \langle B \rangle \langle C \rangle - \langle A \rangle \langle B \rangle \langle C \rangle + \langle C \rangle \langle AB \rangle + 2 \langle AC \rangle + \langle B \rangle \langle AC \rangle - 2 \langle BC \rangle - \langle A \rangle \langle BC \rangle + \langle ABC \rangle$

$(\#10^*)$: $\quad 0 \le 4 + 2 \langle A \rangle \langle B \rangle + 2 \langle C \rangle + 2 \langle B \rangle \langle C \rangle - 2 \langle AB \rangle + \langle C \rangle \langle AB \rangle - 2 \langle AC \rangle + \langle B \rangle \langle AC \rangle + \langle A \rangle \langle BC \rangle - \langle ABC \rangle$

$(\#11^*)$: $\quad 0 \le 4 - 2 \langle B \rangle + \langle B \rangle \langle C \rangle + \langle A \rangle \langle B \rangle \langle C \rangle - 2 \langle AB \rangle + \langle C \rangle \langle AB \rangle - \langle B \rangle \langle AC \rangle - 3 \langle BC \rangle + \langle ABC \rangle$

$(\#12^*)$: $\quad 0 \le 4 - 2 \langle B \rangle + 2 \langle A \rangle \langle C \rangle + \langle B \rangle \langle C \rangle - \langle A \rangle \langle B \rangle \langle C \rangle - 2 \langle AB \rangle + \langle C \rangle \langle AB \rangle - 2 \langle AC \rangle + \langle B \rangle \langle AC \rangle - 3 \langle BC \rangle + \langle ABC \rangle$

$(\#13^*)$: $\quad 0 \le 4 - 2 \langle A \rangle \langle B \rangle - 2 \langle A \rangle \langle C \rangle - \langle B \rangle \langle C \rangle - \langle A \rangle \langle B \rangle \langle C \rangle + 2 \langle AB \rangle - \langle C \rangle \langle AB \rangle + \langle B \rangle \langle AC \rangle + \langle BC \rangle + \langle ABC \rangle$

$(\#14^*)$: $\quad 0 \le 4 - 2 \langle A \rangle \langle B \rangle + 2 \langle A \rangle \langle C \rangle - \langle B \rangle \langle C \rangle + \langle A \rangle \langle B \rangle \langle C \rangle + 2 \langle AB \rangle + \langle C \rangle \langle AB \rangle - 2 \langle AC \rangle + \langle B \rangle \langle AC \rangle + \langle BC \rangle + \langle ABC \rangle$

$(\#15^*)$: $\quad 0 \le 4 + 2 \langle A \rangle \langle C \rangle + \langle B \rangle \langle C \rangle + \langle A \rangle \langle B \rangle \langle C \rangle - \langle C \rangle \langle AB \rangle - 2 \langle AC \rangle - \langle B \rangle \langle AC \rangle + 3 \langle BC \rangle + \langle ABC \rangle$

$(\#16^*)$: $\quad 0 \le 4 - 2 \langle B \rangle + 2 \langle A \rangle \langle C \rangle - 2 \langle AB \rangle + \langle C \rangle \langle AB \rangle - 2 \langle AC \rangle + \langle B \rangle \langle AC \rangle - 2 \langle BC \rangle - \langle A \rangle \langle BC \rangle + \langle ABC \rangle$

$(\#17^*)$: $\quad 0 \le 4 + 2 \langle A \rangle \langle B \rangle + 2 \langle A \rangle \langle C \rangle + 2 \langle B \rangle \langle C \rangle - 2 \langle AB \rangle + \langle C \rangle \langle AB \rangle - 2 \langle AC \rangle + \langle B \rangle \langle AC \rangle - 2 \langle BC \rangle + \langle A \rangle \langle BC \rangle + \langle ABC \rangle$

$(\#18)$: $\quad 0 \le 5 + \langle A \rangle + \langle B \rangle - 2 \langle A \rangle \langle B \rangle + \langle C \rangle + \langle A \rangle \langle C \rangle + \langle A \rangle \langle B \rangle \langle C \rangle + 3 \langle AB \rangle + \langle C \rangle \langle AB \rangle + \langle AC \rangle - \langle B \rangle \langle AC \rangle - 4 \langle BC \rangle$

$(\#19^*)$: $\quad 0 \le 5 + \langle A \rangle + \langle B \rangle + 2 \langle A \rangle \langle B \rangle + \langle C \rangle - 2 \langle A \rangle \langle C \rangle + \langle B \rangle \langle C \rangle - \langle A \rangle \langle B \rangle \langle C \rangle + 3 \langle AB \rangle + \langle C \rangle \langle AB \rangle - \langle AC \rangle + \langle B \rangle \langle AC \rangle - 4 \langle BC \rangle$

$(\#20^*)$: $\quad 0 \le 5 + \langle A \rangle - \langle B \rangle - 2 \langle A \rangle \langle B \rangle + \langle C \rangle - \langle A \rangle \langle C \rangle + \langle B \rangle \langle C \rangle + \langle AB \rangle + \langle C \rangle \langle AB \rangle + 2 \langle AC \rangle - 2 \langle B \rangle \langle AC \rangle - 2 \langle BC \rangle - 2 \langle A \rangle \langle BC \rangle - 2 \langle ABC \rangle$

$(\#21^*)$: $\quad 0 \le 5 + \langle A \rangle + \langle B \rangle + \langle C \rangle - \langle A \rangle \langle C \rangle - \langle B \rangle \langle C \rangle - 2 \langle A \rangle \langle B \rangle \langle C \rangle + \langle AB \rangle + 2 \langle C \rangle \langle AB \rangle + 2 \langle AC \rangle + \langle B \rangle \langle AC \rangle - 2 \langle BC \rangle + \langle A \rangle \langle BC \rangle - \langle ABC \rangle$

$(\#22^*)$: $\quad 0 \le 5 - \langle A \rangle + \langle B \rangle - 2 \langle A \rangle \langle B \rangle + \langle C \rangle - 2 \langle A \rangle \langle C \rangle + 2 \langle B \rangle \langle C \rangle + \langle AB \rangle - 2 \langle C \rangle \langle AB \rangle + \langle AC \rangle - 2 \langle B \rangle \langle AC \rangle - \langle BC \rangle - 2 \langle A \rangle \langle BC \rangle + \langle ABC \rangle$

$(\#23^*)$: $\quad 0 \le 5 + \langle A \rangle + \langle B \rangle - \langle A \rangle \langle B \rangle + \langle C \rangle + 2 \langle B \rangle \langle C \rangle + \langle A \rangle \langle B \rangle \langle C \rangle + 2 \langle AB \rangle - \langle C \rangle \langle AB \rangle + \langle AC \rangle - 2 \langle B \rangle \langle AC \rangle - \langle BC \rangle - 2 \langle A \rangle \langle BC \rangle + \langle ABC \rangle$

$(\#24^*)$: $\quad 0 \le 5 + \langle A \rangle + \langle B \rangle - 2 \langle A \rangle \langle B \rangle + \langle C \rangle - \langle A \rangle \langle C \rangle - \langle B \rangle \langle C \rangle - 2 \langle A \rangle \langle B \rangle \langle C \rangle - \langle AB \rangle + 2 \langle C \rangle \langle AB \rangle + 2 \langle AC \rangle + \langle B \rangle \langle AC \rangle + 2 \langle BC \rangle - \langle A \rangle \langle BC \rangle + \langle ABC \rangle$

$(\#25)$: $\quad 0 \le 6 + 2 \langle A \rangle \langle B \rangle + \langle A \rangle \langle C \rangle + 2 \langle B \rangle \langle C \rangle + \langle A \rangle \langle B \rangle \langle C \rangle - 4 \langle AB \rangle - 2 \langle C \rangle \langle AB \rangle - 3 \langle AC \rangle - \langle B \rangle \langle AC \rangle - 2 \langle A \rangle \langle BC \rangle$

$(\#26)$: $\quad 0 \le 6 - 2 \langle A \rangle + \langle A \rangle \langle B \rangle + 2 \langle C \rangle + \langle A \rangle \langle C \rangle + 2 \langle A \rangle \langle B \rangle \langle C \rangle - 5 \langle AB \rangle - \langle C \rangle \langle AB \rangle - 3 \langle AC \rangle + \langle B \rangle \langle AC \rangle - 2 \langle A \rangle \langle BC \rangle$

$(\#27)$: $\quad 0 \le 6 + 2 \langle A \rangle \langle B \rangle + 2 \langle C \rangle + \langle A \rangle \langle C \rangle + \langle A \rangle \langle B \rangle \langle C \rangle - 4 \langle AB \rangle - 2 \langle C \rangle \langle AB \rangle + 3 \langle AC \rangle + \langle B \rangle \langle AC \rangle - 2 \langle A \rangle \langle BC \rangle$

$(\#28)$: $\quad 0 \le 6 + \langle A \rangle \langle B \rangle + \langle A \rangle \langle C \rangle - 2 \langle B \rangle \langle C \rangle + \langle A \rangle \langle B \rangle \langle C \rangle + \langle AB \rangle + \langle C \rangle \langle AB \rangle - 3 \langle AC \rangle - \langle B \rangle \langle AC \rangle + 2 \langle BC \rangle - 2 \langle A \rangle \langle BC \rangle$

$(\#29)$: $\quad 0 \le 6 + 2 \langle B \rangle + \langle A \rangle \langle B \rangle - 2 \langle A \rangle \langle C \rangle + \langle B \rangle \langle C \rangle - 2 \langle A \rangle \langle B \rangle \langle C \rangle + 3 \langle AB \rangle + \langle C \rangle \langle AB \rangle + 2 \langle B \rangle \langle AC \rangle - 5 \langle BC \rangle + \langle A \rangle \langle BC \rangle$

$(\#30)$: $\quad 0 \le 6 + 2 \langle B \rangle - 2 \langle A \rangle \langle B \rangle + 4 \langle A \rangle \langle C \rangle - \langle B \rangle \langle C \rangle + \langle A \rangle \langle B \rangle \langle C \rangle + 2 \langle AB \rangle + 2 \langle C \rangle \langle AB \rangle - 2 \langle AC \rangle + 2 \langle B \rangle \langle AC \rangle + \langle BC \rangle + \langle A \rangle \langle BC \rangle$

$(\#31)$: $\quad 0 \le 6 + \langle A \rangle \langle C \rangle + 4 \langle B \rangle \langle C \rangle + \langle A \rangle \langle B \rangle \langle C \rangle - 2 \langle AB \rangle - 2 \langle C \rangle \langle AB \rangle - 3 \langle AC \rangle - \langle B \rangle \langle AC \rangle - 2 \langle BC \rangle - 2 \langle ABC \rangle$

$(\#32)$: $\quad 0 \le 7 + \langle A \rangle + \langle B \rangle + \langle A \rangle \langle B \rangle + \langle C \rangle - 2 \langle A \rangle \langle C \rangle + 2 \langle B \rangle \langle C \rangle - \langle A \rangle \langle B \rangle \langle C \rangle + 2 \langle AB \rangle + 3 \langle C \rangle \langle AB \rangle + \langle AC \rangle + 2 \langle B \rangle \langle AC \rangle - 3 \langle BC \rangle - 2 \langle A \rangle \langle BC \rangle + 3 \langle ABC \rangle$

$(\#33)$: $\quad 0 \le 8 + 2 \langle A \rangle \langle B \rangle + 4 \langle A \rangle \langle C \rangle - 2 \langle B \rangle \langle C \rangle + 2 \langle A \rangle \langle B \rangle \langle C \rangle - 2 \langle AB \rangle - \langle C \rangle \langle AB \rangle - 4 \langle AC \rangle + \langle B \rangle \langle AC \rangle - 2 \langle BC \rangle - 3 \langle A \rangle \langle BC \rangle - 3 \langle ABC \rangle$

$(\#34)$: $\quad 0 \le 8 + 2 \langle A \rangle - 2 \langle C \rangle - \langle A \rangle \langle C \rangle + 2 \langle B \rangle \langle C \rangle + 3 \langle A \rangle \langle B \rangle \langle C \rangle - 6 \langle AB \rangle + \langle C \rangle \langle AB \rangle + \langle AC \rangle + 2 \langle B \rangle \langle AC \rangle - 3 \langle A \rangle \langle BC \rangle + \langle ABC \rangle$

$(\#35)$: $\quad 0 \le 8 + 2 \langle A \rangle + \langle A \rangle \langle C \rangle + 2 \langle B \rangle \langle C \rangle + 3 \langle A \rangle \langle B \rangle \langle C \rangle + 6 \langle AB \rangle - \langle C \rangle \langle AB \rangle + \langle AC \rangle - 2 \langle B \rangle \langle AC \rangle - 2 \langle BC \rangle - 3 \langle A \rangle \langle BC \rangle + \langle ABC \rangle$

$(\#36)$: $\quad 0 \le 8 - 2 \langle B \rangle + 2 \langle A \rangle \langle B \rangle - 2 \langle C \rangle - \langle B \rangle \langle C \rangle - 3 \langle A \rangle \langle B \rangle \langle C \rangle + 3 \langle C \rangle \langle AB \rangle - 6 \langle AC \rangle + \langle B \rangle \langle AC \rangle + \langle BC \rangle - 2 \langle A \rangle \langle BC \rangle + \langle ABC \rangle$

$(\#37)$: $\quad 0 \le 8 + 2 \langle B \rangle + \langle A \rangle \langle B \rangle - 2 \langle A \rangle \langle C \rangle - 3 \langle A \rangle \langle B \rangle \langle C \rangle + \langle AB \rangle + 2 \langle C \rangle \langle AB \rangle + 2 \langle AC \rangle + 3 \langle B \rangle \langle AC \rangle - 6 \langle BC \rangle - \langle A \rangle \langle BC \rangle + \langle ABC \rangle$

Linear quantifier elimination is already widely used in causal inference for deriving entropic causal compatibility inequalities [16, 24, 25]. In that task, however, the quantifiers being eliminated are entropies on sets of variables for which one or more is latent. By contrast, the quantifiers being eliminated in the inflation technique are all probabilities on sets of variables all of which are observed (although they are the observed variables of the inflated DAG rather than the original DAG); Appendix F will partly elucidate the relation.

Note that the marginal problem can be solved by computing *either* a convex hull *or* by eliminating quantifiers from linear inequalities. The derivation of entropic inequalities, by contrast, is strictly a linear quantifier elimination task, and cannot be recast as a convex hull problem. As such, while convex hull enumeration tools *are* useful for deriving polynomial inequalities via the inflation technique, they are *not* available for the derivation of entropic inequalities; see Appendix A for further details.

Note that if one does not have a characterization of the facets of the marginal polytope, but only a set of inequalities that contain the marginal polytope but are not tight, one can still apply the prescription described above to derive causal compatibility inequalities from these. We consider an example of such an approach in the next section.

E. Causal compatibility inequalities via Hardy-type inferences from logical tautologies

In the literature on Bell inequalities, it has been noticed that incompatibility with the Bell DAG can sometimes be witnessed by merely looking at which events have zero probability and which events have nonzero probability. In other words, instead of considering the *probability* of a composite outcome, the inconsistency of some marginal distributions can be evident from considering only the *possibility* or *impossibility* of each composite outcome. This insight is originally due to Hardy [30], and versions of Bell's theorem that are based on the violation of such **possibilistic constraints** are known as **Hardy-type paradoxes**. For more background on Hardy-type paradoxes, see Refs. [38, 48–51]; a partial classification of these can be found in Ref. [31].

In this approach, the possibilistic constraints follow from a consideration of *logical relations* that can hold among deterministic assignments to the observed variables. As it turns out, such logical constraints can also be leveraged to derive probabilistic constraints instead of possibilistic ones, as shown in Refs. [41, 52]. These constraints yield a partial solution to the marginal problem. In this section, we demonstrate how to systematically derive all such inequalities for

a given DAG.

We have already provided a simple example of a Hardy-type argument in Sec. III-C, in the logic used to demonstrate that the marginal distributions of Eqs. (15-17) are incompatible with the DAG depicted in Fig. 10. For our present purposes, it is useful to recast the argument of Sec. III-C into a new but manifestly equivalent form.

First, note that for the distribution in question, we have

$$A_2{=}1 \implies C_1{=}0 \tag{46}$$

$$B_2{=}1 \implies A_1{=}0 \tag{47}$$

$$C_2{=}1 \implies B_1{=}0 \tag{48}$$

$$\text{Never} \quad A_1{=}0 \text{ and } B_1{=}0 \text{ and } C_1{=}0. \tag{49}$$

From the last constraint one infers that at least one of A_1, B_1 and C_1 must be 1, which from the three other constraints implies that at least one of A_2, B_2 and C_2 must be 0, so that it is not the case that all of A_2, B_2 and C_2 are 1. Thus Eqs. (46-49) imply

$$\text{Never} \quad A_2{=}1 \text{ and } B_2{=}1 \text{ and } C_2{=}1. \tag{50}$$

However, the DAG of Fig. 10 is such that A_2, B_2, and C_2 have no common ancestor and consequently these variables are marginally independent in any distribution consistent with this DAG. Combining this with the fact that the marginal distribution for each of these three variables has full support implies that A_2, B_2, and C_2 sometimes all take the value 1, which contradicts Eq. (50). What is nice about this form of the reasoning is that the appeal to the causal structure occurs only in the very last step.

We are here interested in recasting the argument in such a way that the appeal to *both* the causal structure *and* the form of the marginal distributions occurs only in the very last step. This is done as follows. The first step of the argument is to note that the following proposition is a logical tautology for binary variables (here, $\wedge$, $\vee$ and $\neg$ denote conjunction, disjunction and negation respectively):

$$\neg[A_2{=}1 \wedge C_1{=}1] \bigwedge \neg[B_2{=}1 \wedge A_1{=}1] \bigwedge \neg[C_2{=}1 \wedge B_1{=}1] \bigwedge \neg[A_1{=}0 \wedge B_1{=}0 \wedge C_1{=}0]$$
$$\implies \neg[A_2{=}1 \wedge B_2{=}1 \wedge C_2{=}1]. \tag{51}$$

The second and final step of the argument notes that the given distribution and the given causal structure imply that the antecedent is true while the consequent is false, so that the distribution and causal structure together imply a contradiction.

In our recasting of the Hardy-type argument, the first step—identifying a logical tautology among valuations of certain subsets of the variables— can be understood as a constraint on marginal *deterministic assignments*, and it is a constraint that follows from logic alone. It is useful to think of this first step as the logical counterpart of a consraint on marginals.

We illustrate this last claim with the example just discussed. It can be cast as a marginal scenario where the contexts are $\{A_2B_2C_2\}$, $\{A_2C_1\}$, $\{B_2A_1\}$, $\{C_2B_1\}$, and $\{A_1B_1C_1\}$. The logical tautology (51) is then a constraint on marginal determinstic assignments for this marginal scenario. To see how to obtain a constraint on marginal *distributions*, we start by rewriting Eq. (51) in its contrapositive form ("and" now implicit in the brackets)

$$[\mathbf{A_2{=}1, B_2{=}1, C_2{=}1}] \implies [\mathbf{A_2{=}1}, C_1{=}1] \vee [\mathbf{B_2{=}1}, A_1{=}1] \vee [\mathbf{C_2{=}1}, B_1{=}1] \vee [A_1{=}0 \wedge B_1{=}0 \wedge C_1{=}0]. \tag{52}$$

Next, we note that if a logical tautology can be expressed as

$$[E_0] \implies [E_1] \vee \ldots \vee [E_n], \tag{53}$$

then by applying the union bound (which asserts that the probability of at least one of a set of events occuring is no greater than the sum of the probabilities of each event occuring), one obtains

$$P(E_0) \leq \sum_{j=1}^{n} P(E_j). \tag{54}$$

Applying the union bound to Eq. (52) in particular yields

$$P_{A_2 B_2 C_2}(\mathbf{111}) \leq P_{A_1 B_1 C_1}(000) + P_{A_1 B_2}(\mathbf{11}) + P_{B_1 C_2}(\mathbf{11}) + P_{A_2 C_1}(\mathbf{11}), \tag{55}$$

which is a constraint on the marginal *distributions*.

Note that this inequality allows one to demonstrate the incompatibility of the marginal distributions of Eqs. (15-17) with the inflated DAG just as easily as one can with the tautology of Eq. (51). It suffices to note that the given distribution and causal structure imply that the left-hand side has nonzero probability (which corresponds to the consequent of Eq. (51) being false) while every term on the right-hand side has zero probability (which corresponds to the antecedent of Eq. (51) begin true). But, of course, the inequality can witness many other incompatibilities in addition to this one.

As another example, consider the marginal problem where the variables are $\{A, B, C\}$, with each being binary, and the contexts are the pairs $\{AB\}$, $\{AC\}$, and $\{BC\}$. The following tautology provides a constraint on marginal deterministic assignments:

$$[\mathbf{A{=}1}, \mathbf{C{=}1}] \implies [\mathbf{A{=}1}, B{=}1] \vee [B{=}0, \mathbf{C{=}1}]. \tag{56}$$

(To see that this is a tautology, simply note that $E \wedge F \implies E \wedge F \wedge (G \vee \neg G) = (E \wedge F \wedge G) \vee (E \wedge F \wedge \neg G) \implies (E \wedge G) \vee (F \wedge \neg G)$.) Applying the union bound, one obtains the following constraint on marginal distributions[14]

$$P_{AC}(\mathbf{11}) \leq P_{AB}(\mathbf{11}) + P_{BC}(\mathbf{01}). \tag{57}$$

In this section, we seek to determine, for any marginal scenario, the set of *all* inequalities that can be derived in this manner. We do so by **enumerating** the full set of constraints on marginal deterministic assignments for the given marginal scenario.

We outline the general procedure using the marginal scenario of Fig. 15, where the full set of variables is $\{A_1, A_2, B_1, B_2, C_1, C_2\}$ and the contexts are $\{A_1 B_1 C_1\}$, $\{A_1 B_2 C_2\}$, $\{A_2 B_1 C_2\}$, $\{A_2 B_2 C_1\}$ and $\{A_2 B_2 C_2\}$, pursuant to Eq. (43). As before, we will express the constraints on marginal deterministic assignments as logical implications with a joint valuation of one of the contexts as the **antecedent** and a disjunction over contexts of joint valuations thereon as the **consequent**. In the following, we explain how to generate *all* such implications which are tight in the sense that the consequent is minimal, i.e., involves as few terms as possible in the disjunction.

First, we fix the antecedant by choosing some context and a joint valuation of its variables. In order to generate all contraints on marginal deterministic assignments, one will have to perform this procedure for *every* context as the antecedent and every choice of joint valuation thereof. For the sake of concreteness, we take the example of $[\mathbf{A_2{=}1}, \mathbf{B_2{=}1}, \mathbf{C_2{=}1}]$ as the antecedent. Each logical implication we consider is required to have the property that any variable that appears in both the antecedent and the consequent must be given the same value in both.

To formally determine all valid consequents, we first consider two hypergraphs. The nodes in the first hypergraph correspond to every possible joint valuation of the variables in a context for every possible context. The hyperedges correspond to every possible joint valuation of all the variables. A hyperedge (joint valuation) contains a node (marginal joint valuation) iff the hyperedge is an extension of the node; for example the hyperedge $[A_1{=}0, \mathbf{A_2{=}1}, B_1{=}0, \mathbf{B_2{=}1}, C_1{=}1, \mathbf{C_2{=}1}]$ is an extension of the node $[A_1{=}0, \mathbf{B_2{=}1}, \mathbf{C_2{=}1}]$. In our example following Fig. 15, this initial hypergraph has $5 \cdot 2^3 = 40$ nodes and $2^6 = 64$ hyperedges.

The second hypergraph is a sub-hypergraph of the first one. We delete from the first graph all nodes and hyperedges which contradict the outcomes supposed by the antecedent. For example, the node $[\mathbf{A_2{=}1}, \mathbf{B_2{=}0}, C_1{=}1]$ contradicts the antecedent $[\mathbf{A_2{=}1}, \mathbf{B_2{=}1}, \mathbf{C_2{=}1}]$. We also delete the node corresponding to the antecedent itself. In our example, this final resulting hypergraph has $2^3 + 3 \cdot 2^1 = 14$ nodes and $2^3 = 8$ hyperedges.

All valid (minimal) consequents are (minimal) **transversals** of this latter hypergraph. A transversal is a set of nodes which has the property that it intersects every hyperedge in at least one node. In order to get implications which are as tight as possible, it is sufficient to enumerate only the minimal transversals. Doing so is a well-studied problem in computer science with various natural reformulations and for which manifold algorithms have been developed [53].

In our example, it is not hard to check that the consequent of

$$
\begin{aligned}
[\mathbf{A_2{=}1}, \mathbf{B_2{=}1}, \mathbf{C_2{=}1}] \quad \implies \quad & [A_1{=}0, B_1{=}0, C_1{=}0] \vee [A_1{=}1, \mathbf{B_2{=}1}, \mathbf{C_2{=}1}] \\
& \vee [\mathbf{A_2{=}1}, B_1{=}1, \mathbf{C_2{=}1}] \vee [\mathbf{A_2{=}1}, \mathbf{B_2{=}1}, C_1{=}1]
\end{aligned}
\tag{58}
$$

---

[14] This inequality is in fact equivalent to Eq. (29).

is such a minimal transversal: every assignment of values to all variables which extends the assignment on the left-hand side satisfies at least one of the terms on the right, but this ceases to hold as soon as one removes any one term on the right.

We convert these implications into inequalities in the usual way via the union bound (i.e., replacing "⇒" by "≤" at the level of probabilities and the disjunctions by sums). For example the constraint on marginal deterministic assignments Eq. (58) translates to the constraint on marginal distributions

$$P_{A_2 B_2 C_2}(\mathbf{111}) \leq P_{A_1 B_1 C_1}(\mathbf{000}) + P_{A_1 B_2 C_2}(\mathbf{111}) + P_{A_2 B_1 C_2}(\mathbf{111}) + P_{A_2 B_2 C_1}(\mathbf{111}). \tag{59}$$

Note that Eq. (59) is a strengthening of Eq. (55). Eq. (59) was used earlier in this article as the starting point of our third example of how to derive a causal compatibility inequality for the Triangle scenario, in Sec. III-C (see Eq. (37)). Because Eq. (58) is the progenitor of this inequality, it can be thought of as the progenitor of the causal compatibility inequality that one derives from it, namely, Eq. (40).

Inequalities on marginal distributions that one derives from hypergraph transversals are generally weaker than those that result from a complete solution of the marginal problem. Nevertheless, many Bell inequalities are of this form, the CHSH inequality among them [52]. So it seems that this method is still sufficiently powerful to generate plenty of interesting inequalities. At the same time, it should be significantly easier to perform in practice than the full-fledged linear (let alone nonlinear) quantifier elimination, even if one does it for every possible antecedent.

In conclusion, linear quantifier elimination is the preferable tool for deriving inequalities for the marginal problem whenever it is computationally tractable; but whenever it is not, then enumerating hypergraph transversals presents a good alternative.

V. FURTHER PROSPECTS FOR THE INFLATION TECHNIQUE

Corollary 5 implies that *any* causal compatibility inequality satisfied by the injectable sets on the inflated DAG can be translated into a causal compatibility inequality for the images of the injectable sets on the original DAG. Consequently *any* technique for deriving causal compatibility inequalities on the inflated DAG can potentially be leveraged by the inflation technique. And, as we noted in Sec. IV, even weak constraints at the level of the inflated DAG can translate into strong constraints at the level of the original DAG.

We here consider two additional possibilities for constraints that might be leveraged by the inflation technique.

A. Using *d*-separation relations of the inflated DAG

In Sec. IV, we considered deriving causal compatibility inequalities on the inflated DAG by a technique wherein one first finds a complete or partial solution to the marginal problem for the pre-injectable sets of the inflated DAG, and then one makes use the ancestral independences in the inflated DAG to factorize the joint distributions on some of the pre-injectable sets.

It is natural to wonder whether one can sometimes make use of facts about the causal structure that go beyond specifying ancestral independences. Indeed, it is standard practice, when deriving compatibility conditions for a DAG, to make use of arbitrary *d*-separation relations among variables: if, in a given DAG, $\boldsymbol{X}$ and $\boldsymbol{Y}$ are *d*-separated by $\boldsymbol{Z}$, then a distribution is compatible with that DAG only if it satisfies the conditional independence relation $\boldsymbol{X} \perp \boldsymbol{Y} | \boldsymbol{Z}$. (The criterion for *d*-separation is explained at length in [1, 3, 11, 13], so we elect not to review it here.) As noted earlier, ancestral independence of $\boldsymbol{X}$ and $\boldsymbol{Y}$ is a special type of *d*-separation of $\boldsymbol{X}$ and $\boldsymbol{Y}$, namely, *d*-separation relative to the null set. Thus the question naturally arises whether the inflation technique can sometimes make use of other *d*-separation relations among sets of observed variables.

Every conditional independence relation can be translated into a nonlinear constraint on probabilities: if $\boldsymbol{X}$ and $\boldsymbol{Y}$ are *d*-separated by $\boldsymbol{Z}$, then we have the conditional independence relation $\boldsymbol{X} \perp \boldsymbol{Y} | \boldsymbol{Z}$, which is most commonly expressed in terms of conditional probabilities as the equality $P_{\boldsymbol{XY}|\boldsymbol{Z}}(\boldsymbol{xy}|\boldsymbol{z}) = P_{\boldsymbol{X}|\boldsymbol{Z}}(\boldsymbol{x}|\boldsymbol{z}) P_{\boldsymbol{Y}|\boldsymbol{Z}}(\boldsymbol{y}|\boldsymbol{z})$ for all $\boldsymbol{x}$, $\boldsymbol{y}$, and $\boldsymbol{z}$. As we generally prefer to work with unconditional probabilities, we rewrite this as follows: If $\boldsymbol{X}$ and $\boldsymbol{Y}$ are *d*-separated by $\boldsymbol{Z}$, then $P_{\boldsymbol{XYZ}}(\boldsymbol{xyz}) P_{\boldsymbol{Z}}(\boldsymbol{z}) = P_{\boldsymbol{XZ}}(\boldsymbol{xz}) P_{\boldsymbol{YZ}}(\boldsymbol{yz})$ for all $\boldsymbol{x}$, $\boldsymbol{y}$, and $\boldsymbol{z}$. Such nonlinear constraints can be incorporated as further restrictions on the sorts of joint distributions consistent with the inflated DAG, supplementing the basic constraints of imposing nonnegativity of probabilities for joint valuations of the observed variables.

For example, in Fig. 3 we find that A_1 and C_2 are *d*-separated by $\{A_2 B_2\}$, and so one can, if one wishes, incorporate the constraint that

$$\forall a_1 a_2 b_2 c_2 : P_{A_1 A_2 B_2 C_2}(a_1 a_2 b_2 c_2) P_{A_2 B_2}(a_2 b_2) = P_{A_1 A_2 B_2}(a_1 a_2 b_2) P_{A_2 B_2 C_2}(a_2 b_2 c_2) \tag{60}$$

Every probability that appears in such an equation, though not defined on an injectable set, can still be expressed as a marginal of the joint distribution over all observed variables. For instance, we can express $P_{A_2 B_2}(a_2 b_2)$ as

$$\forall a_2 b_2 : \ P_{A_2 B_2}(a_2 b_2) = \sum_{a_1 b_1 c_1 c_2} P_{A_1 A_2 B_1 B_2 C_1 C_2}(a_1 a_2 b_1 b_2 c_1 c_2). \tag{61}$$

Upon substituting such relations into Eq. (60), one obtains a family of nonlinear inequalities expressed in terms of the joint distribution over all observed variables. We can then proceed as we did before, eliminating the $P_{A_1 A_2 B_1 B_2 C_1 C_2}(a_1 a_2 b_1 b_2 c_1 c_2)$ from the full system of equalities and inequalities. But now some of the equalities, such as those inferred from Eq. (60), are nonlinear.

Many modern computer algebra systems have functions capable of tackling nonlinear quantifier elimination symbolically[15]. Currently, however, it is generally not practical to perform nonlinear quantifier elimination on large polynomial systems with many quantifiers. It may help to exploit results on the particular algebraic-geometric structure of these particular systems [54].

If one is seeking merely to assess the compatibility of a *given* distribution with the Triangle scenario, then one can avoid the quantifier elimination problem and simply try and solve an existence problem: after substituting the values that the given distribution prescribes for the different valuations of the pre-injectable sets into the system of equalities and inequalities, one must simply determine whether there exist values of the $P_{A_1 A_2 B_1 B_2 C_1 C_2}(a_1 a_2 b_1 b_2 c_1 c_2)$ that satisfy the resulting set of linear and nonlinear constraints. Most computer algebra systems can resolve such *satisfiability* questions quite easily[16].

It is also possible to use a mixed strategy of linear and nonlinear quantifier elimination, such as Chaves [6] advocates. The explicit results of [6] are directly causal implications of the *original* DAG, achieved by applying a mixed quantifier elimination strategy. Perhaps further causal compatibility inequalities might be derivable by applying such a mixed quantifier elimination strategy to inflation DAGs.

B. Using copy-index equivalence relations of the inflated DAG

It follows from the definition of the inflation of a causal model that if two variables in the inflated DAG are copy-index-equivalent, $A_i \sim A_j$, then each depends on its parents in the same fashion as A depends on its parents in the original DAG and hence A_i and A_j have the same dependence on their parents. Formally, from the fact that $A_i \sim A$, we infer that $P_{A_i | \mathsf{Pa}_{G'}(A_i)} = P_{A | \mathsf{Pa}_G(A)}$, and from the fact that $A_j \sim A$, we infer that $P_{A_i | \mathsf{Pa}_{G'}(A_i)} = P_{A | \mathsf{Pa}_G(A)}$ and $P_{A_j | \mathsf{Pa}_{G'}(A_j)} = P_{A | \mathsf{Pa}_G(A)}$ (see Eq. (5)). This implies that for any pair of copy-index-equivalent variables such as A_i and A_j,

$$P_{A_i | \mathsf{Pa}_{G'}(A_i)} = P_{A_j | \mathsf{Pa}_{G'}(A_j)}. \tag{62}$$

By the definition of inflation, the ancestral subgraphs of A_i and A_j are identical, we can conclude that the marginal distributions on A_i and A_j must be equal, $P_{A_i} = P_{A_j}$. In addition, one can sometimes find pairs of contexts, each of which contains *several* variables, such that constraints of the form of Eq. (62) imply that the marginal distributions on these two contexts must be equal.

A few examples illustrate the idea (detailed justifications of the following claims can be found in Appendix B). Consider the pair of contexts $\{A_1 A_2 B_1\}$ and $\{A_1 A_2 B_2\}$ for the marginal scenario defined by the inflated DAG of Fig. 3. Note that neither context corresponds to an injectable set. Nonetheless, because of Eq. (62), we can conclude that in the inflated model these satisfy $P_{A_1 A_2 B_1} = P_{A_1 A_2 B_2}$, or equivalently,

$$\forall a a' b : \ P_{A_1 A_2 B_1}(a a' b) = P_{A_1 A_2 B_2}(a a' b). \tag{63}$$

We can also conclude that in the inflated model these marginal distributions satisfy $P_{A_1 A_2 B_1} = P_{A_2 A_1 B_2}$ (where the order of A_1 and A_2 is different on the two sides of the equation), or equivalently,

$$\forall a a' b : \ P_{A_1 A_2 B_1}(a a' b) = P_{A_1 A_2 B_2}(a' a b). \tag{64}$$

This constraint asserts that the distribution $P_{A_1 A_2 B_2}$ must be symmetric under exchange of A_1 and A_2.

———

[15] For example *Mathematica*™'s `Resolve` command, *Redlog*'s `rlposqe`, or *Maple*™'s `RepresentingQuantifierFreeFormula`, etc.
[16] For example *Mathematica*™ `Reduce`ExistsRealQ` function. Specialized satisfiability software such as SMT-LIB's `check-sat` [55] are particularly apt for this purpose.

Indeed, even if we focus on the single context $\{A_1 A_2\}$, the constraint of Eq. (62) implies a constraint on the marginal distribution $P_{A_1 A_2}$, namely, that it is symmetric under exchange of A_1 and A_2,

$$\forall aa': \ P_{A_1 A_2}(aa') = P_{A_1 A_2}(a'a). \tag{65}$$

Parameters such as $P_{A_1 A_2 B_1}(a_1 a_2 b)$, $P_{A_1 A_2 B_2}(a_1 a_2 b)$ and $P_{A_1 A_2}(a_1 a_2)$ can each be expressed as sums of the $P_{A_1 A_2 B_1 B_2 C_1 C_2}(a_1 a_2 b_1 b_2 c_1 c_2)$, so that equations such as (63), (64) and (65) each define a new equality that can be added to the system of equalities and inequalities that constitute the starting point of the satisfiability problem (if one is seeking to test the compatibility of a given distribution with the inflated DAG) or the quantifier elimination problem (if one is seeking to derive causal compatibility inequalities for the inflated DAG). If any such additional constraints yield stronger constraints at the level of the inflated DAG, then they will also translate into stronger constraints at the level of the original DAG.

The problem of finding pairs of marginal contexts in the inflated DAG for which relations of copy-index-equivalence imply equality of the marginal distributions, and the conditions under which such equalities may yield tighter inequalities, are discussed in Appendix B.

C. Causal inference in quantum theory and in generalized probabilistic theories

Recent work has sought to explore quantum generalizations of the notion of a causal model, termed *quantum causal models* [13, 27]. The causal structures are still represented by DAGs, but (i) whereas classically each latent node of the DAG represents a random variable, quantumly, each latent node represents a quantum system associated to a complex Hilbert space, and (ii) whereas classically the manner in which a node depends causally on its parents is represented by a conditional probability distribution, quantumly, it is represented by a completely-positive trace-preserving linear map.

Note, however, that a quantum causal model is still ultimately in the service of explaining joint distributions over classical variables. These variables represent the settings of preparation procedures and the outcomes of measurements that are used in an experiment on quantum systems, and the statistical distribution over such variables is the only experimental data with which one can confront a given quantum causal model. The basic problem of causal inference for quantum causal models, therefore, concerns the compatibility of a joint distribution over observed classical variables with a given DAG when the model supplementing the DAG is quantum (that is, includes latent nodes that are quantum). If a joint distribution over observed variables is compatible with a given DAG within the framework of quantum causal models, we say that it is *quantumly compatible* with that DAG.

One motivation for studying quantum causal models is that they offer a new perspective on an old problem in the foundations of quantum theory: that of establishing precisely which of the principles of classical physics must be abandoned in quantum physics. Wood and Spekkens [11] showed that Bell's theorem [32] can be leveraged to prove that there exist distributions over observed variables (predicted by quantum theory and observed experimentally [10]) that cannot be accounted for in the Bell scenario under any classical causal model without doing violence to fundamental principles of causal inference such as Reichenbach's principle and the principle that conditional independences should not be fine-tuned (the principle of faithfulness). Quantum causal models, on the other hand, *can* account for these distributions in the Bell scenario. In other words, although these distributions are not *classically* compatible with the Bell scenario, they are *quantumly* compatible with it. Furthermore, such quantum causal explanations suggest [56–58] that quantum theory is perhaps best understood as revising our notions of the nature of unobserved entities, how one represents causal dependencies thereon and incomplete knowledge thereof, while nonetheless *preserving* the spirit of Reichenbach's principle and the principle of no fine-tuning.

Another motivation for studying quantum causal models is a practical one. Violations of Bell inequalities have been shown to constitute resources for information processing [59–61]. To achieve such an advantage, however, it is necessary that a given information processing task can be recast in such a way that the causal structure of the protocol mirrors that of the Bell scenario. Many tasks, however, may not be amenable to being cast in this form. And yet the Bell scenario is not the only DAG for which there is a quantum-classical separation, that is, for which there exist distributions that are quantumly but not classically compatible with the DAG.

It has been shown that such a separation also exists in the bilocality scenario [12, 28] and the triangle scenario [12], and it is likely that there will be many more DAGs for which a quantum-classical separation can be found. The hope, therefore, is that for any DAG where one can identify a quantum-classical separation, the separating distributions may constitute a resource for information processing.

For both foundational and practical reasons, therefore, there is a strong motivation to find examples of DAGs that exhibit a quantum-classical separation. However, this is by no means an easy task. The set of distributions that are quantumly compatible with a given DAG is actually very similar to the set of distributions that are classically compatible

with that DAG [12, 13]. For example, both the classical and quantum sets respect all the conditional independence relations among observed nodes that are implied by the d-separation relations of the DAG [13]. Furthermore, recent work has found that set of distributions that are quantumly compatible with a given DAG satisfy many of the entropic inequalities that hold classically [13, 15, 27]. To date, no quantum-classical separation has been identified where the separation is achieved by a Shannon-type entropic inequality on observed variables that is derived from the Markov conditions on all nodes [12, 62]. Fine-graining the scenario by conditioning on root variables ("settings") leads to a different kind of entropic inequality, and these have proven somewhat quantum-sensitive [24, 63, 64]. Such inequalities are still limited, however, in that they only apply to DAGs that include root nodes that are observed[17], and they still fail to witness cases of classical incompatibility of certain distributions with a given DAG (where the incompatibility is witnessed by stronger techniques) [12, 24].

In addition to quantum generalizations of causal models, one can define generalizations for other operational theories that are neither classical nor quantum, as was done in Henson, Lal and Pusey [13]. Such generalizations are formalized using the framework of *generalized probabilistic theories* (GPTs) [65, 66], a framework that is sufficiently general to describe any operational theory that makes statistical predictions about the outcomes of experiments and respects some weak constraints. Some constraints on compatibility can be proven to apply not only to classical and quantum causal models, but to any theory expressible in this framework. In the terminology of Ref. [13], such constraints on compatibility constitute *theory-independent* limits on correlations. These are of interest because they clarify what any conceivable theory of physics can achieve in a given causal scenario.

Furthermore, by knowing which constraints hold in the GPT framework, one can seek to identify DAGs that exhibit a GPT-classical separation or a GPT-quantum separation, that is, to identify DAGs for which there exist distributions that are GPT compatible but not classically compatible (respectively not quantumly compatible) with the DAG.

Consider GPT-classical separation first. Many examples of DAGs exhibiting such a separation were provided in Ref. [13]. Of the classes of DAGs with six or fewer nodes identified therein as having the potential to be interesting (by not satisfying a sufficient condition for being uninteresting), all but three classes were demonstrated to indeed be interesting. Pienaar [26] recently demonstrated that the three remaining classes are interesting as well. In Appendix C we show how the inflation technique provides an alternative means of demonstrating the interestingness of one of these three classes.

GPT-quantum separations are harder to find. The Bell scenario is known to manifest such a separation, through the work of Tsirelson [35] and Popescu and Rohrlich [36]. The identification of such stronger-than-quantum correlations in the Bell scenario has been a focus of much foundational research in recent years. Traditionally the foundational question has always been: why does quantum theory predict correlations that are *stronger* than one would expect classically? But now there is a new question being asked: why does quantum theory predict correlations that are *weaker* than those predicted by other GPTs? There has been some interesting progress in identifying physical principles that can pick out the precise degree of correlations that are exhibited by quantum theory [67–74]. Further opportunities for identifying such principles would be useful. This motivates a classification of DAGs into those which have a quantum-classical separation, those which have a GPT-quantum separation and those which have both.

The difference between classical, quantum and GPT causal models is the manner in which latent nodes are represented as well as the manner in which the causal influence of a latent node on other nodes is represented. (It shares, however, the feature that the entitites that represent such causal influences mirror the causal structure—for instance, in all cases, the state of a pair of root nodes in the DAG is presumed to factorize.)

Henson, Lal and Pusey[13] were able to identify constraints on compatibility that hold for *any* GPT by avoiding making reference to the latent nodes of the DAG (which are treated differently in different GPTs) and only making reference to the observed variables in the DAG.

The inflation technique also only makes reference to the observed nodes in a DAG. In some cases, the inequalities one thereby derives hold for the GPT notion of compatibility. Indeed, the inequality for the triangle scenario that we presented in Eq. (32) is the probabilistic version of the one that Henson Lal and Pusey derive in their article, and—as we already noted—in this case, their proof technique can be understood as an instance of the inflation technique.

Nonetheless, the inflation technique also yields inequalities that hold only for the *classical* notion of compatibility; it is for this reason that it can be used to derive inequalities that are quantumly violated. For instance, in Example 3 of Sec. III-B and Appendix F, we have shown how the inflation technique can be used to derive Bell inequalities, which clearly admit quantum violations. The inflation technique can be used to derive inequalities of the sort which admit quantum violations for the Triangle scenario as well [75].

It is possible that one could generalize the inflation technique to derive inequalities that can achieve a GPT-quantum separation. This, however, requires a careful definition of a quantum causal model and is beyond the scope of this article. Nonetheless, we will note below in which inflation in the quantum context will differ from its classical counterpart.

———————

[17] Rafael Chaves and E.W. are exploring the potential of entropic analysis based on considering distributions conditioned on *non*-root observed nodes. Jacques Pienaar has alluded to similar considerations as a possible avenues for further research as well [26].

Our main focus here, however, will be to explain what distinguishes applications of the inflation technique that yield inequalities for GPT compatibility from those that yield inequalities for classical compatibility. The distinction rests on a structural feature of the inflated DAG, which we now define.

Definition 6. *A DAG $G' \in$ Inflations$[G]$, is said to contain an* **inflationary fan-out** *if it contains a latent node that has two or more children that are copy-index equivalent.*

The inflations of the triangle DAG that are depicted in Fig. 2 and Fig. 3 contain one or more inflationary fan-outs, as does the inflation of the Bell DAG that is depicted in Fig. 12. On the other hand, the simplest inflation of the triangle DAG that we consider in this article, that of Fig. 5, does not contain any inflationary fan-outs.

In the classical context, for every inflationary fan-out, all of the copy-index-equivalent children of the latent node are required to causally depend on the latent node in precisely the same way as their counterparts in the original DAG did. However, the only maps that can achieve such a duplication of dependencies, known as *broadcasting maps*, are not physically realizable, as was famously shown for quantum theory in Ref. [76] and generalized to GPTs in Ref. [77]. These no-broadcasting results are related to the monogamy of entanglement in quantum theory [78, 79] (see also the discussion of the quantum conditional problem in Ref. [56]). Mathematically, there *are* linear maps that can achieve broadcasting, as shown in [80], but if one used these to define the inflation of a quantum causal model, then distributions over certain sets of variables in the inflated DAG (those containing the children of an inflationary fan-out) might fail to be nonnegative. Such inflations might still be useful as a mathematical tool for ultimately deriving causal compatibility inequalities on the original DAG, but one would need to proceed differently from the way we have proceeded in this article: whereas we have here assumed that all joint valuations of the set of observed variables on the inflated DAG are nonnegative, one could not impose such a constraint for the type of quantum inflation just described. Rather than demanding nonnegativity of the full joint distribution, one could only demand nonnegativity for distributions on sets of variables that did not include multiple children of an inflationary fan-out. Note that the inflated DAG in such cases could not be interpreted as a causal structure. Rather, it would be interpreted as describing multiple different *counterfactual* scenarios within which the causal dependencies are the same.

An analysis along these lines has already been carried out successfully by Chaves *et al.* [27] in the derivation of entropic inequalities that capture quantum compatibility. Although Chaves *et al.* [27] do not invoke the inflation technique, they do seem to employ a similar type of structure to model the conditioning of an observed variable on a "setting" variable, a structure that we would describe as an inflated DAG containing inflationary fan-outs. Chaves *et al.* [27] then take pains to avoid including full joint probability distributions in any of the entropic inequalities they apply to this structure, precisely as we would want to do in constructing inequalities on our inflated DAG, and they successfully derive entropic inequalities for quantum compatibility. But so far, no inequalities polynomial in the probabilities have been derived using this method.

VI. CONCLUSIONS

We have described a new technique for deriving causal compatibility inequalities which we have termed the *inflation* technique. We have shown that many pre-existing techniques for witnessing incompatability and for deriving causal compatibility inequaities can be enhanced by the inflation technique. In particular, it can enhance existing methods regardless of whether these pertain to entropic quantitites, correlators or probabilities. Furthermore, we have shown how a complete or partial solution of the marginal problem for the pre-injectable sets of the inflated DAG can be leveraged to obtain causal compatibility inequalities for the original DAG. These inequalities are not necessarily linear in the probabilities for joint valuations of the observed variables, that is, they are nonlinear or polynomial inequalities. As far as we can tell, our inequalities are not related to the nonlinear causal compatibility inequalities which have been derived specifically to constrain classical networks [19–21], nor to the nonlinear inequalities which account for interventions to a given causal structure [34, 81].

Because our technique is capable of exhibiting the incompatibility of the W-type distribution with the Triangle scenario, while entropic techniques cannot, it follows that our polynomial inequalities are stronger than entropic inequalities in at least some cases (see Example 2 of Sec. III-B).

A single causal structure has unlimited potential inflations. Selecting a good inflation from which strong polynomial inequalities can be derived is an interesting challenge. To this end, it would be desirable to understand how particular features of the original causal structure are exposed when different nodes in the DAG are duplicated. By isolating which features are exposed in each inflation, we could conceivably quantify the causal inference strength of each inflation. In so doing, we might find that inflated DAGs beyond a certain level of variable duplication need not be considered. The multiplicity beyond which further inflation is irrelevant may be related to the maximum degree of those polynomials which tightly characterize a causal scenario. Presently, however, it is not clear how to upper bound either number, or whether finite upper bounds can even be expected.

Causal compatibility inequalities are, by definition, merely *necessary* conditions for compatibility. For some DAGs, the inflation technique is able to derive sufficient conditions as well. This occurs for the Bell scenario, as noted in Appendix F. We currently do not know whether or not the inflation technique can be used to also obtain sufficient conditions for an arbitrary DAG (for instance, by applying the technique to all inflations of a DAG or some finite family of inflations). Some evidence against such sufficiency is that we have not seen a way to use the inflation technique to rederive Pearl's instrumental inequality.

We have described how the inflation technique can enhance the power of many diffferent techniques for deriving causal compatibility inequalities and witnessing incompatibility, by applying the latter technique to the inflated DAG and using Corollary 5 and Lemma 3. The computational difficulty of achieving this enhancement depends on the seed technique. We summarize the computational difficulty of various approaches in Tables I and II.

TABLE I. A comparison of different approaches for deriving constraints on compatibility at the level of the inflated DAG (which can then be translated into constraints on compatibility at the level of the original DAG).

Input from causal structure	General problem → Standard algorithm(s)		Difficulty
Only Ancestral independences among the observed variables	Marginal Problem [Sec. IV-D] i.e. Facet Enumeration	→ Fourier-Motzkin Elimination [82–86], Lexicographic Reverse Search [87]	Hard
	Finding Hardy-type tautologies (*partial* solution of marginal problem) [Sec. IV-E] i.e. identifying hypergraph transversals	→ see Eiter *et al.* [53]	Very easy
Ancestral independences among the observed variables + copy-index equivalence relations [Appendix B]	Linear quantifier elmination	→ Fourier-Motzkin Elimination [82–86], Equality set projection [88, 89]	Hard
All *d*-separation conditions on the observable variables [Sec. V-A]	Real Quantifier Elimination	→ Cylindrical Algebraic Decomposition, see [6]	Very hard

TABLE II. A comparison of different approaches for testing causal compatibility of a given distribution with a given DAG by means of using the inflated DAG. These approaches are all means of witnessing the incompatibility of a given distribution with the inflated DAG.

Input from causal structure	General problem → Standard algorithm(s)		Difficulty
Only ancestral independences among the observed variables without (or with) supplementary copy-index equivalence relations [Appendix B]	Linear Satisfiability of (supplemented) Marginal Problem [Sec. IV-C]	→ Simplex method [90, 91]	Very Easy
All *d*-separation conditions on the observable variables [Sec. V-A]	Nonlinear Satisfiability	→ See [55], and semidefinite relaxations [92]	Easy

We have noted that some of the causal compatibility inequalities we derive by the inflation technique are necessary conditions not only for compatibility with a classical causal model, but also for compatibility with a causal model in *any* generalized probabilistic theory, which includes quantum causal models as a special case.

It would be enlightening to understand the extent to which our (classical) polynomial inequalities for a given DAG can be violated by a distribution arising in a quantum causal model for that DAG, that is, the extent to which our inequalities can exhibit a quantum-classical separation for DAGs other than the Bell scenario. A variety of techniques exist for estimating the amount by which a Bell inequality [93, 94] is violated in quantum theory, but even finding a quantum violation of one of our *polynomial* inequalities presents a new task for which we currently lack a systematic approach. Nevertheless, we know that there exists a difference between classical and quantum also beyond Bell scenarios [12, Theorem 2.16], and we hope that our polynomial inequalities will perform better in witnessing this

difference than entropic inequalities do [13, 27].

Finally, we believe that it may be possible to generalize the inflation technique to derive inequalities that are necessary conditions for the compatibilty of a joint distribution over observed variables with a *quantum* causal model. This may provide an alternative approach to understanding the Tsirelson bound [10].

ACKNOWLEDGMENTS

Appendix A: Algorithms for Solving the Marginal Problem

By solving the marginal problem, what we mean is to determine all the facets of the marginal polytope for a given marginal scenario. Since the vertices of this polytope are precisely the deterministic assignments of values to all variables, which are easy to enumerate, solving the marginal problem is an instance of a **facet enumeration problem**: given the vertices of a convex polytope, determine its facets. This is a well-studied problem in combinatorial optimization for which a variety of algorithms are available [95].

A generic facet enumeration problem takes a matrix of vertices $V \in \mathbb{R}^{n \times d}$, where each row is a vertex, and asks what is the set of points $x \in \mathbb{R}^d$ that can be written as a convex combination of the vertices using weights $w \in \mathbb{R}^n$ that are nonnegative and normalized,

$$\left\{ x \in \mathbb{R}^d \ \middle| \ \exists w \in \mathbb{R}^n : \ x = wV, \ w \geq 0, \ \sum_i w_i = 1 \right\}. \tag{A.1}$$

The oldest-known method for facet enumeration relies on **linear quantifier elimination** in the form of Fourier-Motzkin (FM) elimination [82, 83]. This refers to the fact that one starts with the system $x = wV$, $w \geq 0$ and $\sum_i w_i = 1$, which is the half-space representation of a convex polytope (a simplex), and then one needs to project onto x-space by *eliminating* the variables w to which the existential *quantifier* $\exists w$ refers. The Fourier-Motzkin algorithm is a particular method for performing this quantifier elimination one variable at a time; when applied to Eq. (A.1), it is equivalent to the *double description method* [83, 96]. Linear quantifier elimination routines are available in many software tools[18]. The authors found it convenient to custom-code a linear quantifier elimination routine in *Mathematica*™.

Other algorithms for facet enumeration that are not based on linear quantifier elimination include the following. *Lexicographic reverse search* (LRS) [87], which explores the entire polytope by repeatedly pivoting from one facet to an adjacent one, and is implemented in `lrs`. Equality Set Projection (ESP) [88, 89] is also based on pivoting from facet to facet, though its implementation is less stable[19]. These algorithms could be interesting to use in practice, since each pivoting step churns out a new facet; by contrast, Fourier-Motzkin type algorithms only generate the entire list of facets at once, after all the quantifiers have been eliminated one by one.

It may also be possible to exploit special features of marginal polytopes in order to facilitate their facet enumeration, such as their high degree of symmetry: permuting the outcomes of each variable maps the polytope to itself, which already generates a sizeable symmetry group, and oftentimes there are additional symmetries given by permuting some of the variables. This simplifies the problem of facet enumeration [99, 100], and it may be interesting to apply dedicated software[20] to the facet enumeration problem of marginal polytopes [101–103].

---

[18] For example *MATLAB*™'s `MPT2/MPT3`, *Maxima*'s `fourier_elim`, *lrs*'s `fourier`, or *Maple*™'s (v17+) `LinearSolve` and `Projection`. The efficiency of most of these software tools, however, drops off markedly when the dimension of the final projection is much smaller than the initial space of the inequalities. Fast facet enumeration aided by Chernikov rules [84, 97] is implemented in *porta*, *qskeleton* [98], and *skeleton*.

[19] ESP [86, 88, 89] is supported by `MPT2` but not `MPT3`, and by the (undocumented) option of *projection* in the *polytope* (v0.1.1 2015-10-26) python module.

[20] Such as `PANDA`, `Polyhedral`, or `SymPol`.

Appendix B: Constraints on marginal distributions from copy-index equivalence relations

In Sec. V-B, we noted that every copy of a variable in the inflated DAG has the same probabilistic dependence on its parents as every other copy (see Eq. (62)), and that it follows that for certain pairs of marginal contexts the marginal distributions are necessarily equal. In this section, we describe how to identify such pairs of contexts.

Given sets of nodes U and V in an inflated DAG G', let us say that a map $\varphi : \mathsf{SubDAG}(U) \to \mathsf{SubDAG}(V)$ is a **copy isomorphism** if it is a graph isomorphism[21] between $\mathsf{SubDAG}(U)$ and $\mathsf{SubDAG}(V)$ such that $\varphi(X) \sim X$ for all $X \in U$, meaning that φ maps every node $X \in U$ to a node $\varphi(X) \in V$ that is equivalent to X under dropping the copy index.

Furthermore, we say that a copy isomorphism on the subgraphs of the two contexts, $\varphi : \mathsf{SubDAG}(U) \to \mathsf{SubDAG}(V)$, is an **inflationary isomorphism** whenever it can be extended to a copy isomorphism on their ancestral subgraphs of the two contexts, $\Phi : \mathsf{AnSubDAG}(U) \to \mathsf{AnSubDAG}(V)$. Any copy isomorphism, Φ, on the ancestral subgraphs of the two contexts defines an inflationary isomorphism, φ, on the subgraphs of the two contexts by simply restricting the domain of Φ to $\mathsf{SubDAG}(U)$. So in practice, one can either start with $\varphi : \mathsf{SubDAG}(U) \to \mathsf{SubDAG}(V)$ and try to extend it to $\Phi : \mathsf{AnSubDAG}(U) \to \mathsf{AnSubDAG}(V)$, or start with such a Φ and see whether it restricts to a $\varphi : \mathsf{SubDAG}(U) \to \mathsf{SubDAG}(V)$.

For a pair of contexts U and V, a sufficient condition for equality of their marginal distributions in the inflation is that there exists an inflationary isomorphism between them. Because U and V might themselves contain several variables that are copy-index equivalent (recall the examples of Sec. V-B), it follows that in order to equate the distribution P_U with the distribution P_V in an unambiguous fashion, one needs to specify a correspondence between the variables that make up U and those that make up V. This is exactly the data provided by the inflationary isomorphism φ. This result is summarized in the following lemma.

Lemma 7. *Let the DAG G' be an inflation of the DAG G, and let U and V be contexts in G' (not necessarily distinct). If there exists an inflationary isomorphism $\varphi : \mathsf{SubDAG}(U) \to \mathsf{SubDAG}(V)$, then $P_U = P_{V=\varphi(U)}$ in every inflated causal model.*

Lemma 7 is best illustrated by returning to our example from Sec. V-B which considered the inflation DAG of Fig. 3 and the pair of contexts $U = \{A_1 A_2 B_1\}$ and $V = \{A_1 A_2 B_2\}$.

Consider the map

$$\varphi \; : \; A_1 \mapsto A_1, \qquad A_2 \mapsto A_2, \qquad B_1 \mapsto B_2 \tag{B.1}$$

One easily verifies that this is a copy isomorphism between $\mathsf{SubDAG}(U)$ and $\mathsf{SubDAG}(V)$ because it maps each variable in U to a variable in V that is equivalent up to copy-index and because it trivially implements a graph isomorphism (since neither of these graphs has any edges). There is a unique choice to extend φ to a copy isomorphism $\Phi : \mathsf{AnSubDAG}(U) \to \mathsf{AnSubDAG}(V)$, namely, by having Φ reproduce the action of Eq. (B.1) and implement the following isomorphism between the ancestors

$$\Phi \; : \; X_1 \mapsto X_1, \qquad Y_1 \mapsto Y_1, \qquad Y_2 \mapsto Y_2, \qquad Z_1 \mapsto Z_2. \tag{B.2}$$

Therefore φ is indeed an inflationary isomorphism. From Lemma 7, we then conclude that any inflated model satisfies $P_{A_1 A_2 B_1} = P_{A_1 A_2 B_2}$.

Similarly, the map

$$\varphi' \; : \; A_1 \mapsto A_2, \qquad A_2 \mapsto A_1, \qquad B_1 \mapsto B_2 \tag{B.3}$$

is easily verified to be a copy isomorphism between $\mathsf{SubDAG}(U)$ and $\mathsf{SubDAG}(V)$, and there is again a unique choice to extend φ' to a copy isomorphism $\Phi' : \mathsf{AnSubDAG}(U) \to \mathsf{AnSubDAG}(V)$, by extending Eq. (B.3) with

$$\Phi' \; : \; X_1 \mapsto X_1, \qquad Y_1 \mapsto Y_2, \qquad Y_2 \mapsto Y_1, \qquad Z_1 \mapsto Z_2, \tag{B.4}$$

so that φ' is verified to be an inflationary isomorphism. From Lemma 7, we then conclude that any inflated model also satisfies $P_{A_1 A_2 B_1} = P_{A_2 A_1 B_2}$. (And this in turn implies that for the context $\{A_1 A_2\}$, the marginal distribution satisfies $P_{A_1 A_2} = P_{A_2 A_1}$.)

---

[21] A graph isomorphism is a bijective map between the nodes of one graph and the nodes of another, such that the action of the map transforms the complete *set of edges* defining the first graph into the complete set of edges comprising the second graph.

In order to avoid any possibility of conclusion, we emphasize that one does not infer constraints on the marginal distributions over U and V from the mere existence of a copy isomorphism between the subgraphs of U and V nor from the existence of a copy isomorphism between the ancestral subgraphs of U and V. Rather, such constraints are inferred from the existence of an inflationary isomorphism between the subgraphs, i.e., the existence of a copy isomorphism between the ancestral subgraphs that restricts to a copy isomorphism between the subgraphs.

We emphasize this fact because it might seem, at first glance, that the existence of a copy isomorphism between ancestral subgraphs is *by itself* sufficient for deriving constraints on the marginal distributions. To see why this is not the case, we offer the following example.

Take as the original DAG the instrumental scenario of Pearl [22], and consider the inflation depicted in Fig. 17. Consider the pair of contexts $U = \{X_1 Y_2 Z_1\}$ and $V = \{X_1 Y_2 Z_2\}$ on the inflated DAG. Note that these are clearly not pre-injectable sets.

The ancestral subgraphs for these two contexts are precisely the same, namely the DAG of Fig. 18. This DAG has only the identity map as a graph isomorphism, and therefore this is the unique copy isomorphism between $\mathsf{AnSubDAG}(X_1 Y_2 Z_1)$ and $\mathsf{AnSubDAG}(X_1 Y_2 Z_2)$. But if we restrict the domain of this isomorphism to $\mathsf{SubDAG}(X_1 Y_2 Z_1)$, we clearly do *not* get an isomorphism between $\mathsf{SubDAG}(X_1 Y_2 Z_1)$ and $\mathsf{SubDAG}(X_1 Y_2 Z_2)$ because $Z_1 \mapsto Z_1$ and we require that $Z_1 \mapsto Z_2$. (In fact, there are no copy isomorphisms between $\mathsf{SubDAG}(X_1 Y_2 Z_1)$ and $\mathsf{SubDAG}(X_1 Y_2 Z_2)$ because there are no graph isomorphisms between $\mathsf{SubDAG}(X_1 Y_2 Z_1)$ and $\mathsf{SubDAG}(X_1 Y_2 Z_2)$.)

One can try to make use of Lemma 7 when deriving polynomial inequalities with inflation via solving the marginal problem, by imposing $P_U = P_{\varphi(U)}$ as an additional constraint for every inflationary isomorphism $\varphi : \mathsf{SubDAG}(U) \to \mathsf{SubDAG}(V)$ between sets of observable nodes. This is advantageous to speed up to the linear quantifier elimination, since one can solve each of the resulting equations for one of the unknown joint probabilities and thereby eliminate that probability directly without Fourier-Motzkin elimination.

Moreover, one could also hope that these additional equations would result in tighter constraints on the marginal problem, which would in turn yielder tighter causal compatibility inequalities. However, our computations have so far not revealed any example of such a tightening. In some cases, this lack of impact can be explained as follows. Suppose that $\varphi : \mathsf{SubDAG}(U) \to \mathsf{SubDAG}(V)$ is an inflationary isomorphism which is not just the restriction of a copy isomorphism between the ancestral subgraphs, but even the restriction of a copy automorphism $\Phi' : G' \to G'$ of the entire inflated DAG onto itself; in particular, this assumption implies that Φ' also restricts to a copy isomorphism $\Phi : \mathsf{AnSubDAG}(U) \to \mathsf{AnSubDAG}(V)$ between the ancestral subgraphs. In this case, the irrelevance of the additional constraint $P_U = P_{\varphi(U)}$ to the marginal problem for inflated models can be explained by the following argument.

Suppose that some joint distribution $P_{\mathsf{ObservedNodes}[G']}$ solves the unconstrained marginal problem, i.e., without requiring $P_U = P_{\varphi(U)}$. Now apply Φ' to the variables in $P_{\mathsf{ObservedNodes}[G']}$, switching the variables around, to generate a new distribution $P' = P_{\Phi'(\mathsf{ObservedNodes}[G'])}$. Because the set of marginal distributions that arise from inflated models is invariant under this switching of variables, we conclude that P' is also a solution to the unconstrained marginal problem. Taking the uniform mixture of P and P' is therefore still a solution of the unconstrained marginal problem. But this uniform mixture also satisfies the supplementary constraint $P_U = P_{\varphi(U)}$. Hence the supplementary constraint is satisfiable automatically whenever the unconstrained marginal problem is solvable, which makes adding the constraint irrelevant.

Note that the argument does not apply if the inflationary isomorphism $\varphi : U \to V$ cannot be extended to a copy
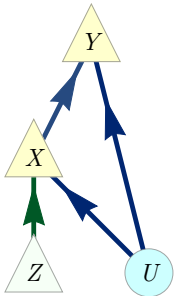

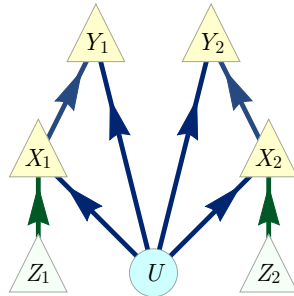FIG. 16. The instrumental scenario of Pearl [22].

FIG. 17. An inflated DAG of the instrumental scenario which illustrates why coinciding ancestral subgraphs doesn't necessarily imply coinciding marginal distributions.
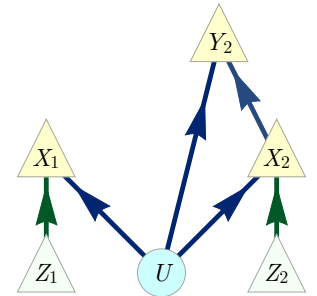
FIG. 18. The ancestral subgraph of Fig. 17 for either $\{X_1 Y_2 Z_1\}$ or $\{X_1 Y_2 Z_2\}$.

automorphism of the entire inflated DAG. It also does not apply if one uses the d-separation conditions beyond ancestral independence on the inflated DAG as additional constraints, because in this case the set of compatible distributions is not necessarily convex. In either of these cases, it is not apparent whether or not constraints arising from copy-index equivalence could yield tighter inequalities.

Appendix C: Using the Inflation Technqiue to Certify a DAG as "Interesting"

By considering all possible d-separation conditions implied by a given DAG, one can infer the set of all conditional independence (CI) relations that must hold in any joint distribution over the observed variables that is compatible with the given DAG. In the presence of nontrivial latent nodes, the set of all *observable* CI relations (that is, CI relations among observed variables) do not always exhaust the constraints on the joint distribution over the observed variables. Henson *et al.* [13] were concerned with identifying DAGs for which an observable distribution satisfying all observable CI relations is *not* a sufficient criterion for compatibility. They introduced the term **interesting** to refer to any DAG which exhibits a discrepancy between the set of observable distributions genuinely compatible with it and the set of observable distributions that merely reproduce its observable CI relations.

Henson *et al.* [13] derived novel necessary criteria on the structure of a DAG in order for it to be interesting, and they conjectured that their criteria may, in fact, be necessary and sufficient. As evidence in favour of this conjecture, they enumerated all possible DAGs with no more than six nodes satisfying their criteria. They found only 21 unique classes of potentially interesting DAGs. Of those 21, they further proved that 18 were unambiguously interesting by writing down an explicit incompatible distribution which nevertheless satisfied the DAGs observable CI relations. Incompatibility of the constructed distribution was certified by means of entropic inequalities.

That left three classes of DAGs as *potentially* interesting. For each of these, Henson *et al.* [13] derived all Shannon-type entropic inequalities in two different ways, once by accounting for non-observable CI relations (that is, CI relations that do not refer exclusively to observed variables) and once without. The existence of *novel* Shannon-type inequalities upon accounting for non-observable CI relations is evidence for the DAG being interesting. The only loophole is that perhaps those novel Shannon-type inequalities are actually non-novel non-Shannon-type inequalities implied by the observable CI relations alone [13].

One way to close this loophole would be to show that the novel Shannon-type inequalities imply constraints beyond some inner approximation to the genuine entropy cone absent non-observable CI relations, perhaps along the lines of Ref. [17]. Another is to use causal compatibility inequalities beyond entropic inequalities to identify some CI-respecting but incompatible distributions. Pienaar [26] accomplished precisely this, and should be credited with the original insight to explicitly consider the different values that an observable root variable might take. In the following, we demonstrate how the inflation technique can be used for this purpose. So far, we have only considered one of the three enigmatic causal structures, namely, Fig. 19.

The following representative causal compatibility inequalities for the DAG of Fig. 19 follow from the inflation technique applied to causal compatibility inequalities for the inflated DAG of Fig. 20, where the latter are obtained from Hardy-type tautologies as described in Sec. IV-E:

$$P_A(0)P_{ADE}(000) \leq P_{AE}(00)P_{AF}(00) + P_A(0)P_{ADF}(001), \tag{C.1}$$

$$P_A(0)P_{ADE}(100) \leq P_{AE}(10)P_{AF}(00) + P_A(1)P_{ADF}(001). \tag{C.2}$$

For example, the second inequality may be explicitly derived as follows. A Hardy-type tautology on the variables of the inflated DAG implies the following constraint on marginals:

$$P_{A_1 A_2 D E_2}(0100) \leq P_{A_1 A_2 F_1 E_2}(0100) + P_{A_1 A_2 D F_1}(0101). \tag{C.3}$$

Applying factorization as per the ancestral independence relations of the inflated DAG, we obtain

$$P_{A_1}(0)P_{A_2 D E_2}(100) \leq P_{A_1 F_1}(01)P_{A_2 E_2}(00) + P_{A_2}(1)P_{A_1 D F_1}(001), \tag{C.4}$$
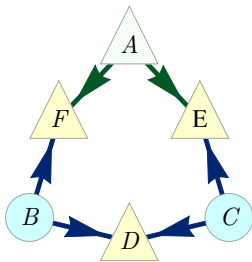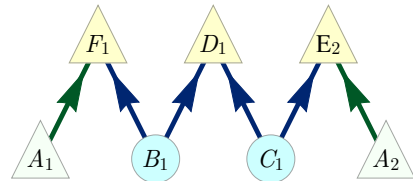

FIG. 19. DAG #15 in Ref. [13].

FIG. 20. A useful inflation of Fig. 19.

and finally translating this into a causal compatibility inequality on the original DAG using Corollary 5, we obtain Eq. (C.2).

In Pienaar [26], it was shown that the following distribution, which is easily verified to satisfy the CI relations among the observed variables of Fig. 19, namely, $A \perp\!\!\!\perp D$ and $E \perp\!\!\!\perp F | A$ [13], is nonetheless incompatible with Fig. 19:

$$P_{ADEF}^{\text{Pien}} := \frac{[0000] + [0101] + [1000] + [1110]}{4}, \quad \text{i.e.} \quad P_{ADEF}^{\text{Pien}}(adef) := \begin{cases} \frac{1}{4} & \text{if } e = a \cdot d \text{ and } f = (a \oplus 1) \cdot d, \\ 0 & \text{otherwise.} \end{cases} \tag{C.5}$$

It is easily verified that this distribution violates the causal incompatibility inequality of Eq. (C.2). It is in this sense that the inflation technique can show that the DAG of Fig. 19 is interesting.

There is another way to see that this distribution is not compatible with Eq. (C.2) using the inflation technique. First, one notes that any marginal distribution on DEF that is compatible with the DAG of Fig. 19 is necessarily also compatible the triangle scenario (where D, E and F are the observed variables). Second, one notes that the marginal distribution P_{DEF}^{Pien} is incompatible with the triangle scenario, since it violates inequality #8 of Sec. IV-D. This is the same inequality which rejects the W-distribution of Eq. (11). Like the W-distribution, the distribution P^{Pien} not only satisfies all Shannon-type entropic inequalities pertinent to Fig. 19, but lies within an inner approximation to the genuine entropy cone for that scenario[22]. In other words, there exists a distribution with the same joint and marginal entropies as P^{Pien} which *is* compatible with Fig. 19.

Finally, it may be worth noting that the inflation of Fig. 20 is precisely the "bilocality scenario" considered by Branciard *et al.* [28]. Therefore, the inflation technique permits us to translate every causal compatibility inequality for the bilocality scenario into a causal compatibility inequality for the DAG of Fig. 19.

---

[22] This is due to Weilenmann and Colbeck (private correspondence).

Appendix D: The Copy Lemma and Non-Shannon type Entropic Inequalities

As it turns out, the inflation technique is also useful outside of the problem of causal inference. As we argue in the following, inflation is secretly what underlies the **Copy Lemma** in the derivation of non-Shannon type entropic inequalities [104, Chapter 15]. The following formulation of the Copy Lemma is the one of Kaced [105].

Lemma 8. *Let A, B and C be random variables with distribution P_{ABC}. Then there exists a fourth random variable A' and joint distribution $P_{AA'BC}$ such that:*

1. *$P_{AB} = P_{A'B}$,*

2. *$A' \perp\!\!\!\perp AC \mid B$.*

The proof via inflation is as follows.

Proof. We begin by noting that every possible joint distribution P_{ABC} is compatible with a DAG of the form of Fig. 21. This follows from the fact that one may take X to be any **sufficient statistic** for the joint variable (A, C) given B, such as $X := (A, B, C)$. Next, we consider the inflation of Fig. 21 depicted in Fig. 22. The maximal injectable sets are $\{A_1 B_1 C_1\}$ and $\{A_2 B_1\}$. By Lemma 3, because P_{ABC} is assumed to be compatible with Fig. 21, it follows that the marginals $\{P_{A_1 B_1 C_1}, P_{A_2 B_1}\}$, where $P_{A_1 B_1 C_1} := P_{ABC}$ and $P_{A_2 B_1} := P_{AB}$, are compatible with the inflated DAG of Fig. 22. The fact that A_2 is d-separated from $A_1 C_1$ by B_1 in Fig. 22 implies that the joint distribution can be expressed as $P_{A_1 A_2 B_1 C_1} := P_{A_1 B_1 C_1} \otimes P_{A_2 B_1} \otimes P_{B_1}^{-1}$, which is only defined for those values of b_1 such that $P_{B_1}(b_1) \neq 0$. By construction, $P_{A_1 A_2 B_1 C_1}$ has $P_{A_1 B_1} = P_{A_2 B_1} = P_{AB}$ and satisfies the conditional independence relation $A_2 \perp\!\!\!\perp A_1 C_1 \mid B_1$. $\qquad\square$

While it is also not hard to write down a distribution with the desired properties explicitly [104, Lemma 15.8], the fact that one can rederive it using the inflation technique is significant. For one, all the non-Shannon type inequalities derived by Dougherty *et al.* [106] are obtained by applying some Shannon type inequality to the distribution that is implied to exist by the Copy Lemma. Our result shows, therefore, that one can understand these non-Shannon type inequalities for a DAG as arising from Shannon-type inequalities applied to an inflation of the DAG. Indeed, it may be that the inflation technique may be a more general-purpose tool for deriving non-Shannon-type entropic inequalities. A natural direction for future research is to explore whether more sophisticated applications of the inflation technique might result in *new* examples of such inequalities.
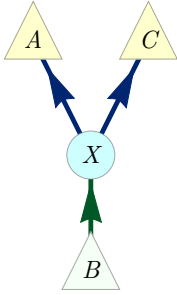

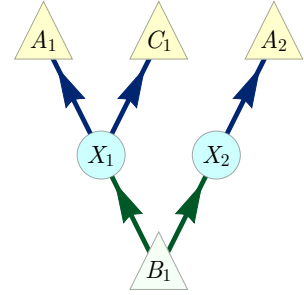FIG. 21. A causal structure that is compatible with any distribution P_{ABC}.

FIG. 22. An inflation of Fig. 21.

Appendix E: Causal compatibility inequalities for the Triangle scenario in machine-readable format

The following polynomial inequalities for the Triangle scenario with binary observed variables have been derived via the linear quantifier elimination method of Sec. IV using the inflated DAG of Fig. 3. Initially this has resulted in 64 symmetry classes of inequalities, where the symmetries are given by permuting the variables and inverting the outcomes. For the resulting 64 inequalities, numerical checks have found violations of only 37 of them: although they are all facets of the marginal polytope over the distributions on pre-injectable sets, there is no guarantee that they are also nontrivial inequalities at the level of the original DAG, and this has indeed turned out not to be the case for 26 of these symmetry classes of inequalities. Moreover, it is still likely to be the case that some of these inequalities are redundant; we have not yet checked whether for every inequality there is a distribution which violates the inequality but satisfies all others.

In the following table, the inequalities are listed in expectation-value form, where we assume the two possible outcomes of each variables to be $\{-1, +1\}$. Each row in the table gives the coefficients with one inequality, which is then ≥ 0. Inequalities $\#'s(1, 3, 4, 8 - 17, 19 - 24)$ in the table are also implied by the hypergraph transversals technique per Sec. IV-E.

TABLE III. List of inequalities as table of coefficients. This is a machine-readable version of the table in Sec. IV-D.

	constant	$\langle A\rangle$	$\langle B\rangle$	$\langle C\rangle$	$\langle AB\rangle$	$\langle AC\rangle$	$\langle BC\rangle$	$\langle ABC\rangle$	$\langle A\rangle\langle B\rangle$	$\langle A\rangle\langle C\rangle$	$\langle B\rangle\langle C\rangle$	$\langle C\rangle\langle AB\rangle$	$\langle B\rangle\langle AC\rangle$	$\langle A\rangle\langle BC\rangle$	$\langle A\rangle\langle B\rangle\langle C\rangle$
(#1):	1	0	0	0	1	1	0	0	0	0	1	0	0	0	0
(#2):	2	0	0	0	0	-2	0	0	0	0	0	-1	0	0	1
(#3):	3	1	-1	1	1	3	0	0	0	0	1	-1	-1	0	1
(#4):	3	1	-1	1	1	3	0	0	0	0	1	1	-1	0	-1
(#5):	3	0	1	0	1	0	-2	0	-1	1	0	1	-1	0	1
(#6):	3	0	1	0	0	-2	-2	0	0	1	0	-1	-1	0	1
(#7):	3	0	1	0	1	0	-2	0	1	-1	0	1	1	0	-1
(#8):	3	1	1	1	2	2	2	-1	1	1	1	1	1	1	-1
(#9):	3	1	1	1	0	2	-2	1	-1	1	1	1	1	-1	-1
(#10):	4	0	0	2	-2	-2	0	-1	2	0	2	1	1	1	0
(#11):	4	0	-2	0	-2	0	-3	1	0	0	1	1	-1	0	1
(#12):	4	0	-2	0	-2	-2	-3	1	0	2	1	1	1	0	-1
(#13):	4	0	0	0	2	-2	1	1	-2	-2	-1	-1	1	0	-1
(#14):	4	0	0	0	2	-2	1	1	-2	2	-1	1	1	0	1
(#15):	4	0	0	0	0	-2	3	1	0	2	1	-1	-1	0	1
(#16):	4	0	-2	0	-2	-2	-2	1	0	2	0	1	1	-1	0
(#17):	4	0	0	0	-2	-2	-2	1	2	2	2	1	1	1	0
(#18):	5	1	1	1	3	1	-4	0	-2	0	1	1	-1	0	1
(#19):	5	1	1	1	3	-1	-4	0	2	-2	1	1	1	0	-1
(#20):	5	1	-1	1	1	2	-2	-2	-2	-1	1	1	-2	-2	0
(#21):	5	1	1	1	1	2	-2	-1	0	-1	-1	2	1	1	-2
(#22):	5	-1	1	1	1	1	-1	1	-2	-2	2	-2	-2	-2	0
(#23):	5	1	1	1	2	1	-1	1	-1	0	2	-1	-2	-2	1
(#24):	5	1	1	1	-1	2	2	1	-2	-1	-1	2	1	-1	-2
(#25):	6	0	0	0	-4	-3	0	0	2	1	2	-2	-1	-2	1
(#26):	6	-2	0	2	-5	-3	0	0	1	1	0	-1	1	-2	2
(#27):	6	0	0	2	-4	3	0	0	2	1	0	-2	1	-2	1
(#28):	6	0	0	0	1	-3	2	0	1	1	-4	1	-1	-2	-2
(#29):	6	0	2	0	3	0	-5	0	1	-2	1	1	2	1	-2
(#30):	6	0	2	0	2	-2	1	0	-2	4	-1	2	2	1	1
(#31):	6	0	0	0	-2	-3	-2	-2	0	1	4	-2	-1	0	1
(#32):	7	1	1	1	2	1	-3	3	1	-2	2	3	2	-2	-1
(#33):	8	0	0	0	-2	-4	-2	-3	2	4	-2	-1	1	-3	2
(#34):	8	2	0	-2	-6	1	0	1	0	-1	2	1	2	-3	3
(#35):	8	2	0	0	6	1	-2	1	0	1	2	-1	-2	-3	3
(#36):	8	0	-2	-2	0	-6	1	1	2	0	-1	3	1	-2	-3
(#37):	8	0	2	0	1	2	-6	1	1	-2	0	2	3	-1	-3

Appendix F: Recovering the Bell inequalities from the inflation technique

To further illustrate the power of our inflated DAG approach, we now demonstrate how to recover all Bell inequalities [9, 10, 32] via our method. To keep things simple we only discuss the case of a bipartite Bell scenario with two values for both "settings" and "outcome" variables here, but the case of more parties and/or more values per variable is totally analogous.

The causal structure associated to the Bell [8–10, 32] experiment [13 (Fig. E#2), 11 (Fig. 19), 24 (Fig. 1), 14 (Fig. 1), 33 (Fig. 2b), 34 (Fig. 2)] is depicted here in Fig. 11. The observable variables are A, B, X, Y, and Λ is the latent common cause of A and B. In a Bell scenario, one traditionally works with the conditional distribution $P_{AB|XY}$, to be understood as an array of distributions indexed by the possible values of X and Y, instead of with the original distribution P_{ABXY}, which is what we do.

In the Bell scenario DAG, the maximal pre-injectable sets are

$$
\begin{aligned}
&\{A_1 B_1 X_1 X_2 Y_1 Y_2\}\\
&\{A_1 B_2 X_1 X_2 Y_2 Y_2\}\\
&\{A_2 B_1 X_1 X_2 Y_2 Y_2\}\\
&\{A_2 B_2 X_1 X_2 Y_2 Y_2\},
\end{aligned}
\tag{F.1}
$$

where notably every maximal pre-injectable set contains all "settings" variables X_1 to Y_2. The marginal distributions on these pre-injectable sets are then specified by the original observable distribution via

$$
\forall abx_1x_2y_1y_2 :
\begin{cases}
P_{A_1 B_1 X_1 X_2 Y_1 Y_2}(abx_1x_2y_1y_2) = P_{ABXY}(abx_1y_1)P_X(x_2)P_Y(y_2),\\
P_{A_1 B_2 X_1 X_2 Y_1 Y_2}(abx_1x_2y_1y_2) = P_{ABXY}(abx_1y_2)P_X(x_2)P_Y(y_1),\\
P_{A_2 B_1 X_1 X_2 Y_1 Y_2}(abx_1x_2y_1y_2) = P_{ABXY}(abx_2y_1)P_X(x_1)P_Y(y_2),\\
P_{A_2 B_2 X_1 X_2 Y_1 Y_2}(abx_1x_2y_1y_2) = P_{ABXY}(abx_2y_2)P_X(x_1)P_Y(y_1),\\
\quad P_{X_1 X_2 Y_1 Y_2}(x_1x_2y_1y_2) = P_X(x_1)P_X(x_2)P_Y(y_1)P_Y(y_2).
\end{cases}
\tag{F.2}
$$

By dividing each of the first four equations by the fifth, we obtain

$$
\forall abx_1x_2y_1y_2 :
\begin{cases}
P_{A_1 B_1|X_1 X_2 Y_1 Y_2}(ab|x_1x_2y_1y_2) = P_{AB|XY}(ab|x_1y_1),\\
P_{A_1 B_2|X_1 X_2 Y_1 Y_2}(ab|x_1x_2y_1y_2) = P_{AB|XY}(ab|x_1y_2),\\
P_{A_2 B_1|X_1 X_2 Y_1 Y_2}(ab|x_1x_2y_1y_2) = P_{AB|XY}(ab|x_2y_1),\\
P_{A_2 B_2|X_1 X_2 Y_1 Y_2}(ab|x_1x_2y_1y_2) = P_{AB|XY}(ab|x_2y_2).
\end{cases}
\tag{F.3}
$$

The existence of a joint distribution over all six variables—i.e. the existence of a solution to the marginal problem—implies in particular

$$
\forall abx_1x_2y_1y_2 : \quad P_{A_1 B_1|X_1 X_2 Y_1 Y_2}(ab|x_1x_2y_1y_2) = \sum_{a',b'} P_{A_1 A_2 B_1 B_2 X_1 X_2 Y_1 Y_2}(aa'bb'|x_1x_2y_1y_2),
\tag{F.4}
$$

and similarly for the other three conditional distributions under consideration. For consistency with the causal hypothesis, therefore, the original distribution must satisfy in particular

$$
\forall ab :
\begin{cases}
P_{AB|XY}(ab|00) = \sum_{a',b'} P_{A_1 A_2 B_1 B_2 X_1 X_2 Y_1 Y_2}(aa'bb'|0101)\\
P_{AB|XY}(ab|10) = \sum_{a',b'} P_{A_1 A_2 B_1 B_2 X_1 X_2 Y_1 Y_2}(a'abb'|0101)\\
P_{AB|XY}(ab|01) = \sum_{a',b'} P_{A_1 A_2 B_1 B_2 X_1 X_2 Y_1 Y_2}(aa'b'b|0101)\\
P_{AB|XY}(ab|11) = \sum_{a',b'} P_{A_1 A_2 B_1 B_2 X_1 X_2 Y_1 Y_2}(a'ab'b|0101)
\end{cases}
\tag{F.5}
$$

The possibility to write the conditional probabilities in the Bell scenario in this form is equivalent to the existence of a latent variable model, as noted in Fine's Theorem [107]. Thus, if an inflated model exists with the required marginals, then a latent variable model of the original distribution exists as well (and conversely, trivially). Hence the inflated DAG of Fig. 12 provides necessary and sufficient conditions for the consistency of the original observed distribution with the Bell scenario causal structure.

Moreover, it is possible to describe the marginal polytope over the pre-injectable sets of Eq. (F.1), due to the fact that the "settings" variables X_1 to Y_4 occur in all four contexts. This description is easier to state for the marginal *cone*, by which we mean the convex cone spanned by the marginal polytope, i.e. the convex cone consisting of all

nonnegative linear combinations of deterministic assignments of values, or equivalently the convex cone of all measures on the set of joint outcomes. This cone lives in $\oplus_{i=1}^4 \mathbb{R}^{2^6} = \oplus_{i=1}^4 (\mathbb{R}^2)^{\otimes 6}$, where each tensor factor has basis vectors corresponding to the two possible outcomes of each variable, and the direct summands enumerate the four contexts. Now the marginal cone is precisely the set of all nonnegative linear combinations of the points

$$(e_{A_1} \otimes e_{B_1} \otimes e_{X_1} \otimes e_{X_2} \otimes e_{Y_1} \otimes e_{Y_2})$$
$$\oplus (e_{A_1} \otimes e_{B_2} \otimes e_{X_1} \otimes e_{X_2} \otimes e_{Y_1} \otimes e_{Y_2})$$
$$\oplus (e_{A_2} \otimes e_{B_1} \otimes e_{X_1} \otimes e_{X_2} \otimes e_{Y_1} \otimes e_{Y_2})$$
$$\oplus (e_{A_2} \otimes e_{B_2} \otimes e_{X_1} \otimes e_{X_2} \otimes e_{Y_1} \otimes e_{Y_2}),$$

where all six variables range over their deterministic outcomes. Since the last four tensor factors occur in every direct summand in exactly the same way, the resulting marginal cone is linearly isomorphic to the cone generated by all vectors of the form

$$[(e_{A_1} \otimes e_{B_1}) \oplus (e_{A_1} \otimes e_{B_2}) \oplus (e_{A_2} \otimes e_{B_1}) \oplus (e_{A_2} \otimes e_{B_2})] \otimes [e_{X_1} \otimes e_{X_2} \otimes e_{Y_1} \otimes e_{Y_2}]$$

in $\mathbb{R}^{2^2} \otimes \mathbb{R}^{2^4}$. Now since the first four variables in the first tensor factor vary completely independently of the latter four variables in the second tensor factor, the resulting cone will be precisely the tensor product [108] of two cones: first, the cone generated by all vectors of the form

$$(e_{A_1} \otimes e_{B_1}) \oplus (e_{A_1} \otimes e_{B_2}) \oplus (e_{A_2} \otimes e_{B_1}) \oplus (e_{A_2} \otimes e_{B_2}),$$

and second the one spanned by all $e_{X_1} \otimes e_{X_2} \otimes e_{Y_1} \otimes e_{Y_2}$. While the latter cone is simply the standard positive cone of $\mathbb{R}^8$, the former cone is the cone generated by the "local polytope" or "Bell polytope" that is traditionally used in the context of Bell scenarios [10, Sec. II.B]. Standard results on tensor products of cones and polytopes [109] therefore imply that our marginal polytope is the tensor product of the Bell polytope, corresponding to the A_1 to B_2 part, with a simplex corresponding to the X_1 to Y_2 "settings" part. This implies that the facets of our marginal polytope are precisely the pairs consisting of a facet of the Bell polytope and a facet of the simplex. For example, in this way we obtain one version of the CHSH inequality as a facet of the marginal polytope,

$$\sum_{a,b,x,y} (-1)^{a+b+xy} P_{A_x B_y X_1 X_2 Y_1 Y_2}(ab0101) \le 2 P_{X_1 X_2 Y_1 Y_2}(0101).$$

Upon using Eq. (F.3), this becomes

$$\sum_{a,b} (-1)^{a+b} \big(P_{ABXY}(ab00) P_X(1) P_Y(1) + P_{ABXY}(ab01) P_X(1) P_Y(0)$$
$$+ P_{ABXY}(ab10) P_X(0) P_Y(1) - P_{ABXY}(ab11) P_X(0) P_Y(0) \big) \le P_X(0) P_X(1) P_Y(0) P_Y(1),$$

so that dividing by the right-hand side results in essentially the conventional form of the CHSH inequality,

$$\sum_{a,b} (-1)^{a+b} \big(P_{AB|XY}(ab|00) + P_{AB|XY}(ab|01) + P_{AB|XY}(ab|10) - P_{AB|XY}(ab|11) \big) \le 2.$$

In conclusion, the inflation technique is powerful enough to get a precise characterization of all distributions consistent with the Bell causal structure, and our technique for generating polynomial inequalities while solving the marginal problem recovers all Bell inequalities.

It is worth noting that the Bell inequalities may also be derived using the hypergraph-transversals / logical-tautologies technique discussed in Sec. IV-E. For example, the inequality

$$P_{A_1 B_1 X_1 Y_1}(1111) P_{X_2}(0) P_{Y_2}(0)$$
$$\le P_{A_1 B_2 X_1 Y_2}(1010) P_{X_2}(0) P_{Y_1}(1) + P_{A_2 B_1 X_2 Y_1}(0101) P_{X_1}(1) P_{Y_2}(0) + P_{A_2 B_2 X_2 Y_2}(1100) P_{X_1}(1) P_{Y_1}(1) \tag{F.6}$$

is a clear precursor of the Bell inequality

$$P_{AB|XY}(11|11) \le P_{AB|XY}(10|10) + P_{AB|XY}(01|01) + P_{AB|XY}(11|00) \tag{F.7}$$

as Eq. (F.7) is obtained from Eq. (F.6) by dividing both sides by $P_{X_1 Y_1 X_2 Y_2}(1100) = P_{X_1}(1) P_{Y_2}(1) P_{X_2}(0) P_{Y_2}(0)$ and then dropping copy indices. On the other hand, Eq. (F.6) follows directly from factorization of preinjectable sets and the tautology

$$[\mathbf{A_1{=}1}, \mathbf{B_1{=}1}, \mathbf{X_1{=}1}, \mathbf{Y_1{=}1}, \mathbf{X_2{=}0}, \mathbf{Y_2{=}0}]$$

$$\implies [\mathbf{A_1{=}1}, B_2{=}0, \mathbf{X_1{=}1}, \mathbf{Y_1{=}1}, \mathbf{X_2{=}0}, \mathbf{Y_2{=}0}] \vee [A_2{=}0, \mathbf{B_1{=}1}, \mathbf{X_1{=}1}, \mathbf{Y_1{=}1}, \mathbf{X_2{=}0}, \mathbf{Y_2{=}0}] \quad \text{(F.8)}$$

$$\vee [A_2{=}1, B_2{=}1, \mathbf{X_1{=}1}, \mathbf{Y_1{=}1}, \mathbf{X_2{=}0}, \mathbf{Y_2{=}0}].$$

[1] J. Pearl, *Causality: Models, Reasoning, and Inference* (Cambridge University Press, 2009).

[2] P. Spirtes, C. Glymour, and R. Scheines, *Causation, Prediction, and Search*, Lecture Notes in Statistics (Springer New York, 2011).

[3] M. Studený, *Probabilistic Conditional Independence Structures*, Information Science and Statistics (Springer London, 2005).

[4] D. Koller, *Probabilistic Graphical Models: Principles and Techniques* (MIT Press, Cambridge, MA, 2009).

[5] C. M. Lee and R. W. Spekkens, "Causal inference via algebraic geometry: necessary and sufficient conditions for the feasibility of discrete causal models," arXiv:1506.03880 (2015).

[6] R. Chaves, "Polynomial Bell inequalities," Phys. Rev. Lett. **116**, 010402 (2016).

[7] D. Rosset and N. Gisin, "Finite local models for all finite correlation scenarios," unpublished (2016).

[8] J. S. Bell, "On the Einstein-Podolsky-Rosen paradox," Physics **1**, 195 (1964).

[9] J. F. Clauser, M. A. Horne, A. Shimony, and R. A. Holt, "Proposed experiment to test local hidden-variable theories," Phys. Rev. Lett. **23**, 880 (1969).

[10] N. Brunner, D. Cavalcanti, S. Pironio, V. Scarani, and S. Wehner, "Bell nonlocality," Rev. Mod. Phys. **86**, 419 (2014).

[11] C. J. Wood and R. W. Spekkens, "The lesson of causal discovery algorithms for quantum correlations: causal explanations of Bell-inequality violations require fine-tuning," New J. Phys. **17**, 033002 (2015).

[12] T. Fritz, "Beyond Bell's theorem: correlation scenarios," New J. Phys. **14**, 103001 (2012).

[13] J. Henson, R. Lal, and M. F. Pusey, "Theory-independent limits on correlations from generalized Bayesian networks," New J. Phys. **16**, 113043 (2014).

[14] T. Fritz, "Beyond Bell's theorem II: Scenarios with arbitrary causal structure," Comm. Math. Phys. **341**, 391 (2015).

[15] R. Chaves and C. Budroni, "Entropic nonsignalling correlations," arXiv:1601.07555 (2015).

[16] R. Chaves, L. Luft, T. O. Maciel, D. Gross, D. Janzing, and B. Schölkopf, "Inferring latent structures via information inequalities," in *Proc. of the 30th Conference on Uncertainty in Artificial Intelligence* (AUAI, 2014) pp. 112–121.

[17] M. Weilenmann and R. Colbeck, "Non-Shannon inequalities in the entropy vector approach to causal structures," personal communication (2016).

[18] J. Åberg, R. Chaves, D. Gross, A. Kela, and K. U. von Prillwitz, "Inferring causal structures with covariance information," poster session, Quantum Networks conference (2016).

[19] A. Tavakoli, P. Skrzypczyk, D. Cavalcanti, and A. Acín, "Nonlocal correlations in the star-network configuration," Phys. Rev. A **90**, 062109 (2014).

[20] D. Rosset, C. Branciard, T. J. Barnea, G. Pütz, N. Brunner, and N. Gisin, "Nonlinear Bell inequalities tailored for quantum networks," Phys. Rev. Lett. **116**, 010403 (2016).

[21] A. Tavakoli, "Bell-type inequalities for arbitrary noncyclic networks," Phys. Rev. A **93**, 030101 (2016).

[22] J. Pearl, "On the testability of causal models with latent and instrumental variables," in *Proc. 11th Conference on Uncertainty in Artificial Intelligence*, AUAI (Morgan Kaufmann, San Francisco, CA, 1995) pp. 435–443.

[23] B. Steudel and N. Ay, "Information-theoretic inference of common ancestors," Entropy **17**, 2304 (2015).

[24] R. Chaves, L. Luft, and D. Gross, "Causal structures from entropic information: geometry and novel scenarios," New J. Phys. **16**, 043001 (2014).

[25] T. Fritz and R. Chaves, "Entropic inequalities and marginal problems," IEEE Trans. Info. Theo. **59**, 803 (2013).

[26] J. Pienaar, "Which causal scenarios are interesting?" arXiv:1606.07798 (2016).

[27] R. Chaves, C. Majenz, and D. Gross, "Information–theoretic implications of quantum causal structures," Nat. Comm. **6**, 5766 (2015).

[28] C. Branciard, D. Rosset, N. Gisin, and S. Pironio, "Bilocal versus nonbilocal correlations in entanglement-swapping experiments," Phys. Rev. A **85**, 032119 (2012).

[29] W. Dür, G. Vidal, and J. I. Cirac, "Three qubits can be entangled in two inequivalent ways," Phys. Rev. A **62**, 062314 (2000).

[30] L. Hardy, "Nonlocality for two particles without inequalities for almost all entangled states," Phys. Rev. Lett. **71**, 1665 (1993).

[31] S. Mansfield and T. Fritz, "Hardy's non-locality paradox and possibilistic conditions for non-locality," Found. Phys. **42**, 709 (2012).

[32] J. S. Bell, "On the problem of hidden variables in quantum mechanics," Rev. Mod. Phys. **38**, 447 (1966).

[33] J. M. Donohue and E. Wolfe, "Identifying nonconvexity in the sets of limited-dimension quantum correlations," Phys. Rev. A **92**, 062120 (2015).

[34] G. V. Steeg and A. Galstyan, "A sequence of relaxations constraining hidden variable models," in *Proc. 27th Conference on Uncertainty in Artificial Intelligence* (AUAI, 2011) pp. 717–726.

[35] B. S. Cirel'son, "Quantum generalizations of Bell's inequality," Lett. Math. Phys. **4**, 93 (1980).

[36] S. Popescu and D. Rohrlich, "Quantum nonlocality as an axiom," Found. Phys. **24**, 379 (1994).

[37] J. Barrett and S. Pironio, "Popescu-rohrlich correlations as a unit of nonlocality," Phys. Rev. Lett. **95**, 140401 (2005).

[38] Y.-C. Liang, R. W. Spekkens, and H. M. Wiseman, "Specker's parable of the overprotective seer: A road to contextuality, nonlocality and complementarity," Phys. Rep. **506**, 1 (2011).

[39] D. Roberts, *Aspects of Quantum Non-Locality*, Ph.D. thesis, University of Bristol (2004).

[40] I. Pitowsky, "George Boole's 'conditions of possible experience' and the quantum puzzle," Br. J. Philos. Sci. **45**, 95 (1994).

[41] I. Pitowsky, *Quantum Probability - Quantum Logic*, Lecture Notes in Physics, Berlin Springer Verlag, Vol. 321 (Springer Berlin Heidelberg, 1989).

[42] H. G. Kellerer, "Verteilungsfunktionen mit gegebenen Marginalverteilungen," Z. Wahrscheinlichkeitstheorie **3**, 247 (1964).

[43] A. J. Leggett and A. Garg, "Quantum mechanics versus macroscopic realism: is the flux there when nobody looks?" Phys. Rev. Lett. **54**, 857 (1985).

[44] M. Araújo, M. Túlio Quintino, C. Budroni, M. Terra Cunha, and A. Cabello, "All noncontextuality inequalities for the n-cycle scenario," Phys. Rev. A **88**, 022118 (2013), arXiv:1206.3212.

[45] S. Abramsky and A. Brandenburger, "The sheaf-theoretic structure of non-locality and contextuality," New J. Phys. **13**, 113036 (2011).

[46] N. N. Vorob'ev, "Consistent families of measures and their extensions," Theory Probab. Appl. **7**, 147 (1960).

[47] T. Kahle, "Neighborliness of marginal polytopes," Beiträge Algebra Geom. **51**, 45 (2010).

[48] A. Garuccio, "Hardy's approach, Eberhard's inequality, and supplementary assumptions," Phys. Rev. A **52**, 2535 (1995).

[49] A. Cabello, "Bell's theorem with and without inequalities for the three-qubit greenberger-horne-zeilinger and *W* states," Phys. Rev. A **65**, 032108 (2002).

[50] D. Braun and M.-S. Choi, "Hardy's test versus the Clauser-Horne-Shimony-Holt test of quantum nonlocality: Fundamental and practical aspects," Phys. Rev. A **78**, 032114 (2008).

[51] L. Mančinska and S. Wehner, "A unified view on Hardy's paradox and the Clauser–Horne–Shimony–Holt inequality," J. Phys. A **47**, 424027 (2014).

[52] G. Ghirardi and L. Marinatto, "Proofs of nonlocality without inequalities revisited," Phys. Lett. A **372**, 1982 (2008).

[53] T. Eiter, K. Makino, and G. Gottlob, "Computational aspects of monotone dualization: A brief survey," Discrete Appl. Math. **156**, 2035 (2008).

[54] L. D. Garcia, M. Stillman, and B. Sturmfels, "Algebraic geometry of Bayesian networks," J. Symbol. Comp. **39**, 331 (2003), arXiv:math/0301255.

[55] C. Barrett, P. Fontaine, and C. Tinelli, "The Satisfiability Modulo Theories Library (SMT-LIB)," www.SMT-LIB.org (2016).

[56] M. S. Leifer and R. W. Spekkens, "Towards a formulation of quantum theory as a causally neutral theory of Bayesian inference," Phys. Rev. A **88**, 052130 (2013).

[57] R. W. Spekkens, "The paradigm of kinematics and dynamics must yield to causal structure," *Questioning the Foundations of Physics: Which of Our Fundamental Assumptions Are Wrong?*, Questioning the Foundations of Physics , 5 (2015).

[58] J. Henson, "Causality, Bell's theorem, and Ontic Definiteness," arXiv:1102.2855 (2011).

[59] J. Barrett, N. Linden, S. Massar, S. Pironio, S. Popescu, and D. Roberts, "Nonlocal correlations as an information-theoretic resource," Phys. Rev. A **71**, 022101 (2005).

[60] V. Scarani, "The device-independent outlook on quantum physics," Acta Physica Slovaca **62**, 347 (2012).

[61] J.-D. Bancal, *On the Device-Independent Approach to Quantum Physics* (Springer International Publishing, 2014).

[62] R. Chaves and T. Fritz, "Entropic approach to local realism and noncontextuality," Phys. Rev. A **85**, 032113 (2012).

[63] S. L. Braunstein and C. M. Caves, "Information-theoretic Bell inequalities," Phys. Rev. Lett. **61**, 662 (1988).

[64] B. W. Schumacher, "Information and quantum nonseparability," Phys. Rev. A **44**, 7047 (1991).

[65] H. Barnum and A. Wilce, "Post-classical probability theory," arXiv:1205.3833 (2012).

[66] P. Janotta and H. Hinrichsen, "Generalized probability theories: what determines the structure of quantum theory?" J. Phys. A **47**, 323001 (2014).

[67] S. Popescu, "Nonlocality beyond quantum mechanics," Nat. Phys. **10**, 264 (2014).

[68] T. H. Yang, M. Navascués, L. Sheridan, and V. Scarani, "Quantum Bell inequalities from macroscopic locality," Phys. Rev. A **83**, 022105 (2011).

[69] D. Rohrlich, "Pr-box correlations have no classical limit," *Quantum Theory: A Two-Time Success Story: Yakir Aharonov Festschrift*, Yakir Aharonov Festschrift , 205 (2014).

[70] M. Pawlowski and V. Scarani, "Information Causality," arXiv:1112.1142 (2011).

[71] A. B. Sainz, T. Fritz, R. Augusiak, J. B. Brask, R. Chaves, A. Leverrier, and A. Acín, "Exploring the Local Orthogonality Principle," Phys. Rev. A **89**, 032117 (2014).

[72] A. Cabello, "Simple explanation of the quantum limits of genuine n-body nonlocality," Phys. Rev. Lett. **114**, 220402 (2015).

[73] H. Barnum, M. P. Müller, and C. Ududec, "Higher-order interference and single-system postulates characterizing quantum theory," New Journal of Physics **16**, 123029 (2014).

[74] M. Navascués, Y. Guryanova, M. J. Hoban, and A. Acín, "Almost quantum correlations," Nat. Commun. **6**, 6288 (2015).

[75] T. C. Fraser and E. Wolfe, "Witnessing uniquely quantum correlations in the triangle scenario," unpublished (2016).

[76] H. Barnum, C. M. Caves, C. A. Fuchs, R. Jozsa, and B. Schumacher, "Noncommuting mixed states cannot be broadcast," Phys. Rev. Lett. **76**, 2818 (1996).

[77] H. Barnum, J. Barrett, M. Leifer, and A. Wilce, "Cloning and broadcasting in generic probabilistic theories," quant-ph/0611295 (2006).

[78] K. A. Dennison and W. K. Wootters, "Entanglement sharing among quantum particles with more than two orthogonal states," Phys. Rev. A **65**, 010301 (2001).

[79] M. Koashi and A. Winter, "Monogamy of quantum entanglement and other correlations," Phys. Rev. A **69**, 022309 (2004).

[80] B. Coecke and R. W. Spekkens, "Picturing classical and quantum Bayesian inference," Synthese **186**, 651 (2011).

[81] C. Kang and J. Tian, "Polynomial constraints in causal bayesian networks," in *Proc. of the 23rd Conference on Uncertainty in Artificial Intelligence* (AUAI, 2007) pp. 200–208.

[82] A. Fordan, *Projection in Constraint Logic Programming* (Ios Press, 1999).

[83] G. B. Dantzig and B. C. Eaves, "Fourier-Motzkin elimination and its dual," J. Combin. Th. A **14**, 288 (1973).

[84] S. I. Bastrakov and N. Y. Zolotykh, "Fast method for verifying Chernikov rules in Fourier-Motzkin elimination," Comp. Mat. & Math. Phys. **55**, 160 (2015).

[85] E. Balas, "Projection with a minimal system of inequalities," Comp. Optimiz. Applic. **10**, 189 (1998).

[86] C. N. Jones, E. C. Kerrigan, and J. M. Maciejowski, "On polyhedral projection and parametric programming," J. Optimiz. Theo. Applic. **138**, 207 (2008).

[87] D. Avis, "A revised implementation of the reverse search vertex enumeration algorithm," in *Polytopes — Combinatorics and Computation*, DMV Seminar, Vol. 29, edited by G. Kalai and G. M. Ziegler (Birkhäuser Basel, 2000) pp. 177–198.

[88] C. Jones, *Polyhedral Tools for Control*, Ph.D. thesis, University of Cambridge (2005).

[89] C. Jones, E. C. Kerrigan, and J. Maciejowski, *Equality set projection: A new algorithm for the projection of polytopes in halfspace representation*, Tech. Rep. (Cambridge University Engineering Dept, 2004).

[90] K. Korovin, N. Tsiskaridze, and A. Voronkov, "Implementing conflict resolution," Perspectives of Systems Informatics , 362 (2012).

[91] F. Bobot, S. Conchon, E. Contejean, M. Iguernelala, A. Mahboubi, A. Mebsout, and G. Melquiond, "A simplex-based extension of Fourier-Motzkin for solving linear integer arithmetic," Automated Reasoning , 67 (2012).

[92] M. Laurent and P. Rostalski, "The approach of moments for polynomial equations," in *Handbook on Semidefinite, Conic and Polynomial Optimization*, edited by M. F. Anjos and J. B. Lasserre (Springer, 2012) pp. 25–60.

[93] M. Navascués, S. Pironio, and A. Acín, "A convergent hierarchy of semidefinite programs characterizing the set of quantum correlations," New J. Phys. **10**, 073013 (2008).

[94] K. F. Pál and T. Vértesi, "Quantum bounds on bell inequalities," Phys. Rev. A **79**, 022120 (2009).

[95] D. Avis, D. Bremner, and R. Seidel, "How good are convex hull algorithms?" Computational Geometry **7**, 265 (1997).

[96] K. Fukuda and A. Prodon, "Double description method revisited," Combinatorics and Computer Science: 8th Franco-Japanese and 4th Franco-Chinese Conference , 91 (1996).

[97] D. V. Shapot and A. M. Lukatskii, "Solution building for arbitrary system of linear inequalities in an explicit form," Am. J. Comp. Math. **02**, 1 (2012).

[98] S. Bastrakov, "qskeleton," sbastrakov.github.io/qskeleton (2016), polyhedral computation software for Fourier-Motzkin elimination with Chernikov rules.

[99] D. Bremner, M. Dutour Sikiric, and A. Schürmann, "Polyhedral representation conversion up to symmetries," in *Polyhedral computation*, CRM Proc. Lecture Notes, Vol. 48 (Amer. Math. Soc., 2009) pp. 45–71, arXiv:math/0702239.

[100] A. Schürmann, "Disc. geom. optim." (Springer International Publishing, Heidelberg, 2013) Chap. Exploiting Symmetries in Polyhedral Computations, pp. 265–278.

[101] V. Kaibel, L. Liberti, A. Schürmann, and R. Sotirov, "Mini-workshop: Exploiting symmetry in optimization," Oberwolfach Rep. , 2245 (2010).

[102] T. Rehn and A. Schürmann, "C++ tools for exploiting polyhedral symmetries," in *Proceedings of the Third International Congress Conference on Mathematical Software*, ICMS'10 (Springer-Verlag, Berlin, Heidelberg, 2010) pp. 295–298.

[103] S. Lörwald and G. Reinelt, "Panda: a software for polyhedral transformations," EURO Journal on Computational Optimization , 1 (2015).

[104] R. W. Yeung, *Information Theory and Network Coding* (Springer US, Boston, MA, 2008) Chap. Beyond Shannon-Type Inequalities, pp. 361–386.

[105] T. Kaced, "Equivalence of two proof techniques for non-Shannon-type inequalities," in *Information Theory Proceedings (ISIT)* (IEEE, 2013) pp. 236–240, arXiv:1302.2994.

[106] R. Dougherty, C. F. Freiling, and K. Zeger, "Non-Shannon information inequalities in four random variables," arXiv:1104.3602 .

[107] A. Fine, "Hidden variables, joint probability, and the Bell inequalities," Phys. Rev. Lett. **48**, 291 (1982).

[108] I. Namioka and R. Phelps, "Tensor products of compact convex sets," Pacific J. Math. **31**, 469 (1969).

[109] T. Bogart, M. Contois, and J. Gubeladze, "Hom-polytopes," Math. Z. **273**, 1267 (2013), arXiv:1111.3880.